

# Calcification and latitudinal distribution of extant coccolithophores across the Drake Passage during late austral summer 2016

5 Mariem Saavedra-Pellitero<sup>1,2</sup>, Karl-Heinz Baumann<sup>1,3</sup>, Miguel Ángel Fuertes<sup>4</sup>, Hartmut Schulz<sup>5</sup>, Yann Marcon<sup>1,3</sup>, Nele Manon Vollmar<sup>1</sup>, José-Abel Flores<sup>4</sup>, Frank Lamy<sup>6</sup>

<sup>1</sup> Department of Geosciences, University of Bremen, PO Box 33 04 40, 28334 Bremen, Germany.

<sup>2</sup> School of Geography, Earth and Environmental Sciences, University of Birmingham, UK.

<sup>3</sup> MARUM, Center for Marine Environmental Sciences, University of Bremen, 28359 Bremen, Germany.

10 <sup>4</sup> Departamento de Geología, Universidad de Salamanca, 37008 Salamanca, Spain.

<sup>5</sup> Mathematisch-Naturwissenschaftliche Fakultät, University of Tübingen, Hölderlinstr. 12, 72074 Tübingen, Germany.

<sup>6</sup> Alfred Wegener Institute for Polar and Marine Research, Am Alten Hafen 26, D-27568, Bremerhaven, Germany.

*Correspondence to:* Mariem Saavedra-Pellitero (msaavedr@uni-bremen.de)

## 15 **Abstract:**

Coccolithophores are globally distributed microscopic marine algae that exert a major influence on the global carbon cycle through calcification and primary productivity. There is recent interest in coccolithophore polar communities, however field observations regarding their biogeographic distribution are scarce for the Southern Ocean. This study documents the latitudinal, as well as in depth, variability in the coccolithophore assemblage composition and the coccolith mass variation of the ecologically dominant *Emiliania huxleyi* across the Drake Passage. Ninety-six water samples were taken between 10 and 150 m water depth from 18 stations during POLARSTERN Expedition PS97 (February-April, 2016). A minimum of 200 coccospores per sample were identified in scanning electron microscope and coccolith mass was estimated with light microscopy. We find that coccolithophore abundance, diversity and maximum depth habitat decrease southwards marking different oceanographic fronts as ecological boundaries. We characterize three zones: (1) the Chilean margin, where *E. huxleyi* type A (normal and overcalcified) and type R are present; (2) the Subantarctic Zone (SAZ), where *E. huxleyi* reaches maximum values of  $212.5 \times 10^3$  cells/L and types B/C, C, O are dominant. (3) The Polar Front Zone (PFZ), where *E. huxleyi* types B/C and C dominate. We link the decreasing trend in *E. huxleyi* coccolith mass to the poleward latitudinal succession from type A to type B group. Remarkably, we find that coccolith mass is strongly anticorrelated to total alkalinity, total CO<sub>2</sub>, bicarbonate ion and pH. We speculate that low temperatures are a greater limiting factor than carbonate chemistry in the Southern Ocean. However, further in situ oceanographic data is needed to verify the proposed relationships. We hypothesize that assemblage composition and calcification modes of *E. huxleyi* in the Drake Passage will be strongly influenced by the ongoing climate change.

## 1. Introduction

5 The carbon chemistry of the ocean has a fundamental impact on marine life. The current influx of anthropogenic CO<sub>2</sub> into the surface ocean is causing a substantial perturbation to marine chemistry, as exhibited by variations in alkalinity, carbonate ion, saturation state or pH (e.g., Gattuso et al., 2011). Many organisms use dissolved inorganic carbon for photosynthesis and/or the production of calcium carbonate biominerals. Open ocean phytoplankton includes coccolithophore algae, a unicellular organism belonging to the phylum Haptophyta (Young and Bown, 1997; Young et al., 2003). Within a single coccolithophore cell there are  
10 dual pathways of carbon utilization – for photosynthesis and for biomineralization of calcium carbonate platelets, called coccoliths. Coccolithophores produce up to ~40% of open ocean calcium carbonate (Poulton et al., 2013) and are responsible for ~20% of global net marine primary production (Malone et al., 2017). Therefore, how coccolithophore respond to changing oceanic conditions is of upmost importance for marine ecology and carbon cycling. The ratio between particulate organic carbon formed during photosynthesis and particulate inorganic carbon produced via calcification varies depending on species or even morphotypes  
15 within species (Blanco-Ameijeiras et al., 2016), but can also be highly influenced by environmental conditions, such as seawater CO<sub>2</sub> concentration, total alkalinity, and phosphate concentration (Findlay et al., 2011). As climate varies, it is expected that these key conditions will change, and it is predicted that upper oceans may experience increased stratification and decreased nutrient availability in the upper photic zone (Cabré et al., 2015). How exactly coccolithophores will respond to these changes is subject to debate.  
20

Ocean acidification combined with the increase in sea-surface temperature due to global warming are major concerns in polar and subpolar regions (e.g., Wassmann et al., 2011; Post et al., 2013; Freeman and Lovenduski, 2015), triggering an increasing interest in coccolithophore ecology at high latitudes (e.g., Harada et al., 2012; Dylmer et al., 2015; Balch et al., 2016; Charalampopoulou et al., 2016; Giraudeau et al., 2016; Saruwatari et al., 2016; Nissen et al., 2018; Rigual Hernández et al., 2018; Krumhardt et al.,  
25 2019). Questions remain about how coccolithophore populations will adapt to predicted changes in their environment, if at all. There is growing concern that increasing levels of CO<sub>2</sub> in the atmosphere and the subsequent acidification of the ocean may disrupt the production of coccoliths. As more of the water column becomes undersaturated in CaCO<sub>3</sub> in the future (Fabry et al., 2009), carbonate dissolution will be favored over precipitation and coccolithophores may be less successful in exporting carbon to the deep ocean (Fabry et al., 2008). Additionally, any change in the global distribution and abundance of coccolithophore species  
30 relative to non-calcifying groups of phytoplankton (e.g., naked Haptophyceae cells, diatoms, etc) will have important effects on the biogeochemical cycling of carbon and climatic feedbacks. A known positive correlation exists over long timescales between surface-ocean carbonate ion concentrations [CO<sub>3</sub><sup>2-</sup>] and the mean coccolith mass of the associated Noëlaerhabdaceae assemblage, a family of coccolithophores, which includes the extant species *Emiliania huxleyi* (Beaufort et al., 2011). This correlation is driven by the replacement of more- by less-heavily calcified morphotypes or species with declining [CO<sub>3</sub><sup>2-</sup>]. Although the physiological  
35 driver for this strong ecological selective pressure is not known (Beaufort et al., 2011), it may determine Noëlaerhabdaceae biogeography, particularly in high latitudes, both in the past and future (Cubillos et al., 2007).

Geographical shifts in the occurrence or abundance of coccolithophores and assemblage compositions have been recently observed (e.g., Rivero-Calle et al., 2015; Krumhardt et al., 2016). Repeated sampling in the Australian sector of the Southern Ocean (SO) over the past four decades has shown a dramatic range expansion of *E. huxleyi* south of 60°S (Cubillos et al., 2007), where any ocean acidification effect appears outweighed by surface-ocean warming. Other authors also recorded a southward expansion of the habitat of *E. huxleyi* in the SO during the last two decades (Winter et al., 2014), although the actual cause of this latitudinal expanse is still under debate (e.g., Patil et al., 2014; Malinverno et al., 2015). Even with a temperature-driven range expansion of coccolithophores in the SO, surface ocean carbonate chemistry is now capable of exerting a first-order control on the composition of coccolithophore assemblages as well as on overall coccolithophore calcification (Cubillos et al., 2007; Mohan et al., 2008; Beaufort et al., 2011; Freeman and Lovenduski, 2015).

10

With significant changes in marine species distributions already occurring, it is crucial to understand the ecosystem structure as well as the potential impact of environmental change on the provision of essential ecosystem services (O'Brien et al., 2016). In this work, we assess the potential relationship between environmental parameters and the community composition, biogeography and calcification mode of modern high latitude coccolithophore communities across the Drake Passage. Accordingly, we calculated extant coccolithophore species numbers at different stations between 10 and 150 m of the water column, evaluated the coccolith mass variations of *E. huxleyi*. We compared these observations with in situ conductivity-temperature-depth (CTD) measurements, carbonate chemistry parameters, as well as to previously published Southern Ocean coccolithophore and calcification datasets.

## 2. Material and methods

### 2.1. Sample preparation for scanning electron microscope analyses and coccolithophore taxonomical considerations

20 Ninety-six water samples were taken at 18 stations located in the southern Chilean continental margin and across the western end of the Drake Passage (Fig. 1) from February to April 2016 during Expedition PS97 (Lamy, 2016). Seawater samples were obtained at different depths using a rosette sampler with 24 × 12 L Niskin bottles (Ocean Test Equipment Inc.) attached to a CTD Seabird SBE911 plus device (Lamy, 2016). The bottles were fired by a SBE32 carousel. For the study of coccolithophore assemblages, 4 to 7 samples per station, between 10 and 150 m water depth, were chosen. Two litres of water were filtered onto 0.45 µm pore size 25 Polycarbonate Track-Etch Membrane, air-dried and stored over silica gel. A small part of the filter was cut out, fixed on an aluminum Scanning Electron Microscope (SEM) stub and sputtered with gold/palladium. A specific area of the center of the filter was analysed with Zeiss DSM 940A SEM at the University of Bremen, to determine quantitative cell counts for all morphotypes, species and total coccolithophore abundance at magnifications of 1000x, 2000x and 5000x when required. A minimum of 200 whole coccospores per sample were counted and classified following Young et al. (2003), the revised classification of Jordan et al. (2004) and the electronic guide to the biodiversity and taxonomy of coccolithophores Nannotax 3 (ina.tmsoc.org/Nannotax3/index.html) by Young et al. (2019).

30 Initially, seven different morphotypes of *Emiliania huxleyi* were distinguished in the study area belonging to two main groups, types A and B (for further details see Nannotax). These are type A (*huxleyi*), type A overcalcified, type B (*pujosiae*), type B/C, type C (*kleijneae*), type R and type O (which included specimens with an opened central area and specimens with the central area covered by a thin plate) (Table 1, Plate 1). Additionally, the degree of calcification was visually assessed while counting, that is why the terms “normal”, “calcified” and “heavily calcified” are used in this work to denote some of the most robust *E. huxleyi* placoliths regardless the morphotype (see Plate 1). Semiquantitative estimates of preservation were based on SEM observations

on the coccolithophore assemblage. “Good” preservation implied little or no evidence of carbonate dissolution. Coccoliths with the main morphological characteristics partially altered but still identifiable at species level were tagged as “moderate” (e.g., T-elements within the taxon *E. huxleyi* were present). Specimens affected by strong dissolution or high fragmentation were regarded as “poor” (e.g., T-elements within the taxon *E. huxleyi* were dissolved).

5

## 2.2. Oceanographic data

The CTD-rosette hydrocasts during Expedition PS97 (Lamy, 2016) provided vertical water column profiles of in situ sea surface temperature (SST), salinity (SSS), density, oxygen and fluorescence (reflecting chlorophyll-a concentrations) (Fig. 2). According to the criteria specified by Orsi et al. (1995), different oceanographic fronts were crossed in this latitudinal transect, the Subantarctic 10 Front (SAF) between stations PS97/036-1 and PS97/037-1 and the Antarctic Polar Front (PF), at PS97/040-1 (Fig. 1). The areas between these fronts are referred to as Subantarctic Zone (SAZ), north of the SAF, Polar Front Zone (PFZ), between the SAF and PF and Antarctic Zone (AZ), south of the PF.

Phosphate, nitrate and silicate contents were retrieved from the World Ocean Atlas 2013 (WOA13)  $1^\circ \times 1^\circ$  grid austral summer 15 collection (December to February) (Garcia et al., 2014). Total carbon dioxide ( $T_{CO_2}$ ) and total alkalinity ( $T_{ALK}$ ) values were obtained from the Ocean Data View (ODV) global alkalinity and total dissolved carbon  $1^\circ \times 1^\circ$  grid collection from the uppermost 150 m of the water column during austral summer (December to February) (Goyet et al., 2000). Since carbonate chemistry parameters were not measured in situ and data availability in the Drake Passage/Southern Ocean is limited, bicarbonate ion ( $HCO_3^-$ ), carbonate ion ( $CO_3^{2-}$ ), saturation state ( $\Omega_{Ca}$ ) and pH were calculated (as derived variables) with ODV software version 4.6.3 20 (Schlitzer, 2015) using the uppermost 150 m of the GLODAPv2 collection (Key et al., 2015) and excluding measurements done before 1980.  $HCO_3^-$ ,  $CO_3^{2-}$ ,  $\Omega_{Ca}$  and pH were also calculated (for comparison purposes) using the CO2SYS.XLS program for 10-20 m depth (Pierrot et al., 2006) and considering the interpolated values of  $T_{ALK}$ ,  $T_{CO_2}$  and nutrients as well as the in situ measurement of temperature, salinity and pressure.

25 The values of each of these oceanographic parameters were estimated at the location of every CTD station by interpolating the available data points. The interpolation used a triangulation-based linear method for CTD stations located within the boundaries of the available data, and a nearest neighbour extrapolation method for any CTD stations located outside of the data boundaries. Latitude/longitude coordinates were projected to Universal Transverse Mercator (Zone 19E, World Geodetic System 1984) before interpolation in order to minimize the distance distortion inherent in geographic coordinates. The calculations were done in 30 MATLAB<sup>TM</sup> using a custom function that is provided as supplementary material.

## 2.3. Sample preparation and coccolith calcite estimates in light microscope

Fifteen samples were selected in a latitudinal transect for coccolith calcite estimates, between 10 and 20 m water depth. Sample preparation was designed and carried out at the University of Salamanca (Spain). A part of the filter (ca. 1/4 of the original Polycarbonate Track-Etch Membrane) was cut out and carefully placed into small plastic bags. Buffered water (pH = 9) was 35 prepared with 0.075g/L of  $Na_2CO_3$ , 0.1 g/L and 0.04g/L of unflavored gelatin (“Gold Gelatin”). Six hundred  $\mu L$  of buffered water were added, and the bags were sealed consistently in a triangular shape. After 30 minutes, the bags were shaken in a lab vortex for 3 minutes to ensure that coccoliths were fully detached from the filter and re-suspended. Holding each bag on top of a cover slide placed on a hot plate (ca. 60°C), an incision was made with a scalpel in one of the bag angles, allowing the solution to slowly drop

onto the cover slide. Once the water was evaporated, the cover slip was mounted with mixture of 50% Canada balsam and 50% Xylene and left in an oven (40° C) for at least 24h. This technique ensured that coccoliths were in the same plane of focus for polarized light microscopy. The dried filter was checked for presence/absence of coccoliths later on in the SEM of the University of Bremen (see supplementary material).

5

In this study, a Nikon Eclipse LV100 POL polarized light microscope with a 100x H/N2 objective set-up with circular polarization was used at the University of Salamanca. In order to determine coccolith mass and thickness, between 20 and 53 random fields of view were imaged using the Nikon DS-Fi1 digital 8-bit colour camera and the NisElements software, keeping the light level of the microscope and aperture settings constant. The images were processed with the C-Calcita software (for further details see Fuertes 10 et al., 2014). Calibration was done with images of a well preserved and in-focus calcareous spine from the sample PS97/033-1 at 10 m (see supplementary material). In total, 796 coccoliths were analysed, with a minimum of 34 coccoliths (up to 94) measured per sample.

## 2.4. Diversity indices

15 The Shannon index ( $H$ ), the Simpson diversity index ( $1-D$ ) and the Fisher's alpha index were calculated with Paleontological Statistics (PAST™) software version 3.22 (Hammer et al., 2001) using the raw coccolithophore counts.  $H$  was determined with the following equation (1):

$$H = - \sum_i \frac{n_i}{n} \ln \frac{n_i}{n} \quad (1)$$

where  $n_i$  is the number of individuals in taxon  $i$ , and  $n$  is the total number of all individuals. This index takes into account the 20 number of individuals as well as the number of taxa.  $H$  ranges from 0 for communities with just one taxon to higher values for communities with many taxa, each with few individuals (Harper, 1999). Dominance,  $D$ , was determined with the equation (2):

$$D = \sum_i \left( \frac{n_i}{n} \right)^2 \quad (2)$$

The Simpson index  $1-D$  varies from 0 to 1 and measures evenness of the community. Fisher's alpha was calculated with the following equation (3):

$$S = a * \ln(1 + n/a) \quad (3)$$

where  $S$  is number of taxa,  $n$  is number of individuals and  $a$  is the Fisher's alpha.

## 2.5. Statistics

A principal component analysis (PCA) was performed on the coccolithophore relative abundance data using PAST™ software 30 version 3.22 (Hammer et al., 2001). The objective of the PCA is to find hypothetical variables, called components, that capture the maximum proportion of the variance in the multivariate dataset as possible (Davis, 1986; Harper, 1999). These new variables are linear combinations of the original variables (Hammer et al., 2001). The first principal component has the largest variance possible, and each subsequent component explains the next greatest variance possible. Samples in which less than 50 coccospores were 35 counted were excluded from the original database, therefore just 74 samples were considered for the PCA. In order to avoid skewness, the relative abundances of the different coccolithophore taxa ( $x$ ) were log-transformed prior to the PCA using the formula:  $y = \log(x+1)$ . This transformation enhanced the importance of rare taxa, and minimized the dominance of few abundant taxa (Mix et al., 1999), in this case of *E. huxleyi* types B/C and C.

Seventeen coccolithophore taxa were considered for the PCA (see the taxonomical groups in Table 2). Due to the similar ecological preferences observed, *Papposphaera* sp. and *Pappomonas* spp. were lumped together in one taxonomical group, in the same way as holococcolithophores, the *Syracosphaera* and the *Ophiaster* species (Table 2). In contrast, *E. huxleyi* morphotypes were regarded as different groups. A correlation matrix between the principal component scores and the environmental variables (i.e., SST, SSS, fluorescence, oxygen and density measured in situ, as well as nitrate, phosphate and silicate contents interpolated from the WOA13) was performed in order to identify potential relationships between the environmental parameters and the coccolithophore components.

## 10 3. Results

### 3.1. Coccolithophore distribution

The analysis of 96 water samples shows in general higher cell concentrations in the uppermost 100 m of the water column in the SAZ and at shallower depths (ca. 60 m) in the PFZ (Fig. 3 a). The highest coccolithophore number,  $214.6 \times 10^3$  cells/L, is reached at station PS97/034-2 (60 m) in SAZ, but high cell concentrations are generally observed north of the SAF (Fig. 3 a). The uppermost 150 m average of coccolithophore concentrations drastically drop at the oceanographic fronts, from  $119.9 \times 10^3$  to  $56.4 \times 10^3$  cells/L (PS97/036-1, /037-1) at the SAF, and from  $32.2 \times 10^3$  to  $0.1 \times 10^3$  cells/L (PS97/040-1, /041-1) at the PF. Stations south of the PF show very low cell numbers or are devoid of coccolithophores, but detached coccoliths are occasionally observed at the southernmost locations, even at station PS97/50-2. Coccolithophore preservation is in general moderate to good north of the PF, with optimum values at 10-20 m, but becomes notably poorer in the AZ (Fig. 3 c).

20

### 3.2. Coccolithophore community composition

Twenty-three different coccolithophore taxa (including morphotypes) are observed in this transect across the Drake Passage (Table 2). The most dominant species is *E. huxleyi*, although less abundant taxa also dwell in these (sub-) polar waters. In the following lines, we will comment on the main species composing the coccolithophore community, from the dominant taxa to the rare ones.

#### 25 3.2.1. *Emiliania huxleyi*

*Emiliania huxleyi* dominates the coccolithophore assemblage, reaching values up to  $212.5 \times 10^3$  cells/L at PS97/034-2 (60 m). This taxon is present in all the stations, except at coccolithophore-barren samples south of the PF, where coccospores are occasionally recorded in low numbers, always below  $3.0 \times 10^3$  cells/L. Seven well established morphotypes of *E. huxleyi* are observed; these are types A, A overcalcified, B, B/C, C, R and O (Plate 1), grouped into A (Fig. 4) and B (Fig. 5) according to Young et al. (2019). 30 Neither malformed *E. huxleyi*, morphotype D, nor var. *corona* are present in the studied samples. However, a variation in the degree of coccolithophore calcification is observed; i.e., heavily calcified specimens as well as weakly calcified specimens are present in this transect (Table 1, Plate 1).

35 *Emiliania huxleyi* A group is less abundant than group B and includes type A, type A overcalcified and type R, all of them present in coastal waters (Fig. 4 a). Type R (Plate 1 a) is the most uncommon *E. huxleyi* morphotype, and it just dwells offshore Chile and at station PS97/038-1 (20 m), where it reaches a maximum of  $0.9 \times 10^3$  cells/L (Fig. 4 c). A similar distribution pattern is shown by *E. huxleyi* type A overcalcified (Fig. 4 d, Plate 1 b, c), with concentrations up to  $1.8 \times 10^3$  cells/L at PS97/018-1 (100 m). *Emiliania*

*huxleyi* type A (normal form or moderately calcified, Plate 1 d-f) is restricted to the continental margin, where it records numbers of up to  $1.8 \times 10^3$  cells/L (Fig. 4 b).

*Emiliania huxleyi* B group specimens dwell north of the PF, showing a broader distribution than A group (Fig. 5 a); it includes types B, B/C, C and O. Type B (Plate 1 g-i) is the most unusual *E. huxleyi* morphotype within group B, with maximum numbers of  $7.4 \times 10^3$  cells/L at PS97/029-1 (10 m). *Emiliania huxleyi* type B is abundant in a narrow deep band (0-150 m) at the Chilean margin/open ocean transition in the SAZ, and it is occasionally present in shallow waters of the PFZ (Fig. 5 b). Types B/C and C (Plate 1 j-l) show a broader latitudinal distribution and they are the most abundant *E. huxleyi* taxa with maxima of  $74.0 \times 10^3$  cells/L at PS97/030-1 (150 m) and  $103.2 \times 10^3$  cells/L at PS97/034-2 (60 m), respectively (Table 2, Fig. 5 c, d). Type B/C reaches higher concentrations at shallower depths (10-20 m), when compared to type C (20-100 m). Type O, with an “opened” central area (Plate 1 m), displays a similar distribution pattern to type B/C and reaches the highest numbers ( $8.0 \times 10^3$  cells/L at PS97/032-1, 10 m) mainly at shallow depths (10-20 m) (Fig. 5 e). On the contrary, type O with a central area covered by a thin “lamella”, which is highly variable in size, is notably more abundant and dwells at deeper depths (ca. 0-100 m), with maximum abundances of  $72.0 \times 10^3$  cells/L at PS97/036-1, 60 m (Fig. 5 f). *Emiliania huxleyi* detached coccoliths were not counted but their presence or absence was assessed during the SEM analyses. Free detached coccoliths of *E. huxleyi* types B/C-C show a broader distribution than coccospores and are rarely recorded up to 61.7°S at station PS97/050-2.

### 3.2.2. Other taxa

On top of *E. huxleyi*, less abundant taxa are observed. *Ophiaster* spp., including *O. hydroideus* (Plate 2) and sporadically *O. reductus*, is present primarily at the Chilean margin to a maximum 150 m water depth, but unexpectedly reaches up  $10.1 \times 10^3$  cells/L at PS97/038-1 at a depth of 10 m north of the PF (Fig. 6 a). *Calciopappus caudatus* is found in the uppermost 60 m of the SAZ and PFZ with maximum abundances of  $5.3 \times 10^3$  cells/L also at PS97/038-1, 10 m (Fig. 6 b). Four species belonging to the genus *Syracosphaera* are recorded in the Drake Passage (i.e., *S. dilatata*, *S. corolla*, *S. marginaporata* and *S. pulchra*). *Syracosphaera* spp. dominates among the rare coccolithophore assemblage in the SAZ, except at coastal stations, and its highest numbers (up to  $5.3 \times 10^3$  cells/L PS97/038-1) are recorded between 10 and 60 m (Fig. 6 c). In contrast, *Calcidiscus* s.l., mainly *Calcidiscus leptoporus*, displays moderate numbers at the coastal stations offshore Chile (from 10 to 150 m), but reaches higher numbers (up to  $1.4 \times 10^3$  cells/L at PS97/038-1, 10 m) southwards in a rather patchy, but shallow distribution (Fig. 6 d). *Papposphaera* sp. and *Pappomonas* spp. (including sp. 1 and sp. 5) are observed mainly in the PFZ or at shallow depths in the SAZ, with a maximum concentration of  $1.4 \times 10^3$  cells/L at PS97/038-1, 10 m (Fig. 6 e). Holococcolithophores, mainly *Syracosphaera strigilis* HOL (Plate 2), are restricted to the uppermost 60 m in the SAZ with maximum values of  $1.0 \times 10^3$  cells/L (PS97/038-1) (Fig. 6 f).

Rare coccolithophore taxa (maximum below  $0.8 \times 10^3$  cells/L) are also recorded in the Drake Passage. *Gephyrocapsa muellerae* is restricted to the northernmost stations offshore of Chile, while *Chrysotila* sp. is occasionally observed in the SAZ and *Calciosolenia murrayi* in the PFZ (Fig. 7 c-e). *Acanthoica quattrospina* and *Wigwamma antarctica* display a broader distribution, even south of the PF, in the case of the latter (Fig. 7 a, b). Additionally, non-coccolithophores haptophytes belonging to the genera *Petasaria* and *Chrysochromulina* are generally present in the SAZ, PFZ and AZ, reaching maximum concentrations of  $7.8 \times 10^3$  cells/L at PS97/037-1 at 60 m water depth (Fig. 7 f).

In order to investigate the relationship between the coccolithophore composition and the environmental variables in the study area, a PCA, was performed using the data from 74 sampling points (Fig. 8). Based on the broken stick method, the PCA indicates the

existence of three main principal components (PC) explaining 77.4% of the total variance (see supplementary material). PC1 explains 45.3% of the variance and it is positively related to the abundance of *E. huxleyi* type O and negatively related to *E. huxleyi* type C. PC2, connected to *E. huxleyi* type B/C, in a lesser extent to type B, and negatively correlated to *E. huxleyi* type A, accounts for 17.3% of the variance. PC1 seems associated to a marked temperature gradient. Positive PC1-values are linked to 5 warm/moderately warm water taxa, which dwell north of the SAF, and negative PC1-values are connected to taxa that live in colder waters at higher latitudes. PC1 is correlated to SST and anticorrelated to density, oxygen content, macronutrients (phosphate, nitrate) and silicate (Table 3). PC2 is related to salinity variations (Table 3). Negative values of PC2 are related to extant coccolithophore taxa observed in the low salinity waters offshore Chile or to taxa living in the PFZ. On the contrary, positive 10 values of PC2 are linked to taxa dwelling in the SAZ, where the SSS values are the highest of the studied transect. The coccolithophore assemblage composition separates out three different clusters in the PCA (Fig. 8) corresponding to three different oceanographic areas. The SAZ is characterized by positive values PC1 and PC2, the PFZ by negative PC1 and PC2 values, and the Chilean coastal environment (Chl) by positive PC1 and negative PC2.

### 3.3. Diversity

Coccolithophore diversity indices (Shannon index *H*, Simpson index 1-D, Fisher's alpha) as well as the number of taxa are highest 15 offshore Chile (0-150 m) and they became restricted to the uppermost 60 m in the PFZ (Fig. 9). The number of taxa is maximal at station PS97/038-1 (10 m) and drastically drops south of the PF. The Shannon and Simpson 1-D indices display a similar pattern (Fig. 9 b, d), are highly correlated ( $r=0.95$ , supplementary material) and show that coccolithophore diversity decreases southwards. The number of taxa and diversity indices are strongly related to latitude (Fig. 9 c, f), with station PS97/038-1 (10-20 m) being an outlier due to the high diversity estimates recorded there.

### 20 3.4. Coccolith calcification –*E. huxleyi*

*Emiliania huxleyi* specimens were classified into non-standardized sub-categories (e.g., regarding level of coccolith calcification) while counting in the SEM. Specimens of type A calcified/heavily calcified and overcalcified (Fig. 10 a) are present at the same locations as the common *E. huxleyi* type A (Fig. 4). Calcification in the group B implied in most of the cases a thicker central tube in the coccolith central area and thicker T-elements (Plate 1). Although type B calcified is recorded with rather low numbers, it 25 shows a similar distribution to type B/C calcified (Fig. 10 b, c); both are restricted to the uppermost 150 m of the water column at stations PS97/029-1, /030-1 and /031-1. Type C calcified is occasionally recorded where types B and B/C are present, but shows a much broader and patchy distribution north of the PF (Fig. 10 d).

Coccolith mass measured with the software C-Calcita ranges from 19.8 to 0.8 pg, and median values (per station) vary from 7.3 to 2.4 pg. Relatively high *E. huxleyi* masses are recorded in the SAZ (Fig. 11), but not at the stations with the highest cell 30 concentrations (such as PS97/034-2). Measurements of the coccolith mass allowed us to compare to the identified morphotypes. In general, coccolith mass decreases southwards across the Drake Passage (Fig. 11). While high coccolith masses are reached offshore Chile (i.e., stations PS97/017-1, /018-1) where *E. huxleyi* types R and A (overcalcified) are present, low coccolith masses are reached in the PFZ where types B/C and C dominate (i.e., stations PS97/037-1, /040-1). The gradual latitudinal mass decrease 35 is occasionally interrupted by sudden drops in the mass estimates. These decreases in mass estimates appeared to be controlled by the predominance of a specific morphotype, for instance the low *E. huxleyi* mass values recorded at PS97/016-1 coincide with a sudden increase in the relative abundance of *E. huxleyi* type C (Fig. 11).

## 4. Discussion

### 4.1. Latitudinal variations in the coccolithophore abundance, distribution and diversity.

The observed maximum coccolithophore abundance recorded (up to  $214.6 \times 10^3$  cells/L) is in agreement with previous studies carried out in different sectors of the Southern Ocean, which estimated maximum numbers between 130 and  $640 \times 10^3$  cells/L (e.g., 5 Eynaud et al., 1999; Findlay and Giraudeau, 2000; Cubillos et al., 2007; Gravalosa et al., 2008; Mohan et al., 2008; Hinz et al., 2012; Saavedra-Pellitero et al., 2014; Malinverno et al., 2015; Balch et al., 2016; Charalampopoulou et al., 2016). The coccolithophore abundance, diversity and maximum depth habitat drastically drop from North to South and portray the oceanographic fronts as ecological boundaries. Marked shifts in the coccolithophore numbers, community composition and diversity occurring at the SAF and PF observed here, were also previously noted by other authors in different sectors of the 10 Southern Ocean (e.g., Eynaud et al., 1999; Gravalosa et al., 2008; Saavedra-Pellitero et al., 2014; Malinverno et al., 2015; Balch et al., 2016; Charalampopoulou et al., 2016). Although the aforementioned studies reported increases in the abundance of 15 coccolithophores at the SAF and PF, we only observe an increase in the number of cells/L in the PF at shallow depths (< 60 m, Fig. 3), which is not so evident in the SAF. The increase in coccolithophore abundance recorded in the PF could be linked to the high biological productivity occurring at the Antarctic Circumpolar Current fronts (e.g., Murphy, 1995; Pollard et al., 2002; Patil et al., 2013) due to the frontal dynamics itself (e.g., Laubscher et al., 1993) or to the physical accumulation of particulate matter 20 and nutrients at these convergence zones (e.g., Franks, 1992; Eynaud et al., 1999; Gravalosa et al., 2008; Balch et al., 2016).

The southernmost extent of *E. huxleyi* has been extensively discussed (e.g., Winter et al., 2014; Malinverno et al., 2015). The PF 25 constitutes a natural sharp barrier which marks a drop in coccolithophore diversity and number of coccospores (Saavedra-Pellitero et al., 2014; Saavedra-Pellitero and Baumann, 2015). Several studies observed the absence of *E. huxleyi* south of the PF (e.g., Verbeek, 1989; Charalampopoulou et al., 2016). However, specimens of *E. huxleyi* and *W. antarctica* are sporadically recorded south of the PF in the studied transect with numbers of  $<3 \times 10^3$  cell/L in the uppermost 80 m of the water column at stations PS97/043-3 and /047-1. *Emiliania huxleyi* is observed in low numbers at temperatures between 1.7 and -0.7°C (Fig. 2), below the 30 2°C isotherm limit that McIntyre and Bé (1967) originally established for the Atlantic Southern Ocean. Although it is unusual, few authors occasionally found *E. huxleyi* also dwelling in cold waters < 2°C (see Table 1 in Holligan et al., 2010). Monospecific assemblages of *E. huxleyi* have been also recorded south of the PF by other authors in the Pacific sector (e.g., Gravalosa et al., 2008; Saavedra-Pellitero et al., 2014), Australian sector (e.g., Nishida, 1986; Findlay and Giraudeau, 2000; Cubillos et al., 2007; 35 Malinverno et al., 2015), in the Atlantic sector (e.g., Eynaud et al., 1999; Holligan et al., 2010) and Indian sector (e.g., Mohan et al., 2008; Patil et al., 2014). We speculate that the free detached coccoliths of *E. huxleyi* observed in our study area, down to 61.7°S, and showing a broader distribution than coccospores, are not in situ and could have been transported. In any case the southernmost extent of coccolithophores is also influenced by the clear dominance of diatoms south of the PF, as suggested by the high diatom concentration (valves/g dry sediment) and biogenic opal content recorded in surface sediment samples from the AZ of the Drake Passage (Cárdenas et al., 2018) and from Pacific Southern Ocean extant plankton studies (e.g., Saavedra-Pellitero et al., 2014; 40 Malinverno et al., 2016).

35

The number of taxa and coccolithophore diversity decreases southwards (Fig. 9) in agreement with other studies performed in the Drake Passage, the Australian and Pacific sectors of the Southern Ocean (e.g., Findlay and Giraudeau, 2000; Gravalosa et al., 2008; Saavedra-Pellitero et al., 2014; Charalampopoulou et al., 2016). Coccolithophore diversity is related to the temperature gradient, as shown by the correlation between Shannon index and SST ( $r=0.8$ , see supplementary material). Contrary to Saavedra-Pellitero et al. (2014), the highest coccolithophore diversity values do not always occur at stations that showed the highest coccolithophore 45

abundances (Figs. 3, 9). Few studies offshore Chile (ca. 33°S, 36°S) and in the Drake Passage showed low coastal coccolithophore diversity increasing towards open ocean regions (Charalampopoulou et al., 2016; Menschel et al., 2016; von Dassow et al., 2018) which contrasts with the high number of taxa recorded in this work at uppermost 100 m of the water column at the Chilean margin (Fig. 9). Amongst different environmental factors, temperature could be one of the main variables favouring high coccolithophore diversity at the coastal stations.

The unexpected high diversity and number of taxa recorded at 10-20 m at station PS97/038-1 (previously labelled as “outlier”), coincident with relatively high density of coccospheres, does not seem to have been promoted by high SSTs, but rather by an occasional variation in the nutrient availability. So far, there are no nutrient measurements in situ available for this transect, but the interpolated values from the WOA13 austral summer suggest that nutrients are generally available this part of the SAZ, and shallow (10, 20 m) nitrate or phosphate concentrations (Fig. 12 h, i) do not abruptly change at PS97/038-1. Therefore this could be due to mesoscale eddies which could have advected nutrients (Frenger et al., 2018). We speculate that an increase in the fluorescence values (Fig. 2), reflecting higher chlorophyll-a concentrations, could be attributed to a higher availability of nutrients, which could have favored coccolithophores. The available fluorescence data (Fig. 2) seem to primarily reflect diatom concentration, south of the PF, followed by the non-coccolithophore haptophytes (*Petasaria* and *Chrysochromulina* spp.) in the SAZ and PFZ (up to 100 m water depth) superimposed to the coccolithophore distribution. Future quantitative analyses of extant diatoms and nutrients performed at the same stations and depths are envisaged and will be required for better understanding of the phytoplankton community interactions and ecological patterns across the Drake Passage.

#### 4. 2. Community composition across the Drake Passage.

Based on the PCA (Fig. 8) it was possible to distinguish three main different oceanographic areas, characterized by different coccolithophore assemblages in the study area.

(1) The Chilean margin. Coccolithophores dwell up to 150 m water depth in this zone (Fig. 3). *Emiliania huxleyi* type A is present in the stations closest to the Chilean coast (i.e., PS97/018-1 and /017-1), which recorded the highest SST and lowest SSS in the study area. This morphotype of *E. huxleyi* has been also observed in low abundances north of the SAF in different Pacific/Australian Southern Ocean (e.g., Cubillos et al., 2007; Saavedra-Pellitero et al., 2014; Malinverno et al., 2015), although was not observed by others authors (e.g., Gravalosa et al., 2008; Charalampopoulou et al., 2016), probably due to the high latitudes of those transects. Specimens of type A with different degree of calcification were present ranging from normal to overcalcified (Plate 1), the latter being more abundant. In the Northern Hemisphere, *E. huxleyi* type A dominates the coccolithophore assemblage in the North Atlantic and in Norwegian coastal waters (e.g., van Bleijswijk et al., 1991; Holligan et al., 1993), but not in the Southern Ocean (e.g., Cook et al., 2011; Hagino et al., 2011). *Emiliania huxleyi* type R was observed for first time in the Drake Passage, although it has been previously observed off New Zealand (Langer et al., 2009; Iglesias-Rodriguez et al., 2017) and in the Eastern South Pacific (Beaufort et al., 2008; Beaufort et al., 2011; von Dassow et al., 2018).

Other minor taxa present in the Chilean margin are *Calcidiscus* s.l., *Ophiaster* spp and *G. muellerae*. The first has already been found by other authors in the SAZ (e.g., Saavedra-Pellitero et al., 2014; Malinverno et al., 2015), but its patchy distribution north of the PF is in agreement with observations by Charalampopoulou et al. (2016). *Ophiaster* spp. shows uneven distribution in the

SAZ and PFZ, but it is also present in the Chilean continental margin. *Ophiaster* spp. is recorded offshore Chile with low number living up to 100 m water depth, which contrast the high numbers observed in the SAZ offshore New Zealand always above 60 m (Saavedra-Pellitero et al., 2014). Occasional low numbers of extant *G. muellerae* have also been observed in the Southern Ocean by Saavedra-Pellitero et al. (2014) and Findlay and Giraudeau (2000).

5

(2) The SAZ. This oceanographic zone is bounded in the south by the SAF. Salinity values are relatively constant at about 34 psu, but SST gradually decreases, down to ca. 6° C, while the nitrate and phosphate contents progressively increase (Figs. 2, 12). The SAZ is characterized by the dominance of *E. huxleyi* types C, B/C, O and B. The maximum coccolithophore depth habitat progressively decreases southwards from 150 m in the transitional zone south of the chilean margin to 100 m in the open ocean (Fig. 3). The shift in occurrence from type A group to type B group has been recorded by some authors at the STF in the Australian sector (e.g., Hiramatsu and De Deckker, 1996; Findlay and Giraudeau, 2000; Malinverno et al., 2015). *Emiliania huxleyi* type B appears in very low abundance, in agreement with Saavedra-Pellitero et al. (2014), restricted to a transitional narrow deep band (0-150 m) between the Chilean coastal margin and more open conditions of the SAZ. It has been observed also north of the STF in the Indian Southern Ocean (Patil et al., 2013). This morphotype was otherwise only found in the Northern Hemisphere (Cook et al., 2011).

10

15

*Emiliania huxleyi* type O was established by Hagino et al. (2011), who observed this morphotype extensively distributed in the Southern Ocean. However, so far only Malinverno et al. (2015) and this study described *E. huxleyi* type O. This would mean that the reported geographic distributions of types B/C and C might be biased by inclusion of Type O (Hagino et al., 2011). *Emiliania huxleyi* type O (including the opened and lamella forms) is abundant in the SAZ, which is in agreement with Malinverno et al. (2015). *Emiliania huxleyi* type B/C and C (see Table 1) are the dominant taxa in the SAZ of the Southern Ocean (e.g., Findlay and Giraudeau, 2000; Cubillos et al., 2007; Gravalosa et al., 2008; Mohan et al., 2008; Saavedra-Pellitero et al., 2014; Saavedra-Pellitero and Baumann, 2015).

25

30

Among minor taxa, *Syracosphaera* spp., *Calcidiscus* sp., *A. quattrospina* as well as holococcolithophores are found in the SAZ, in agreement with the assemblage observed by Charalampopoulou et al., (2016) north of the PF. Four species belonging to the genus *Syracosphaera* (plus *S. strigilis* HOL) are recorded in the study area, as previously observed (Gravalosa et al., 2008; Charalampopoulou et al., 2016). *Acanthoica quattrospina*, a species tolerant to low salinity (Supraha et al., 2014) is present in southern high latitudes (Eynaud et al., 1999; Findlay and Giraudeau, 2000; Malinverno et al., 2015), but has not been recorded in other polar transects (e.g., Mohan et al., 2008).

35

40

(3) The PFZ. This oceanographic zone is bounded by the SAF and the PF. Salinity and SST gradually decrease with respect to the SAZ, and nutrient contents continue to progressively increase poleward (Figs. 2, 12). The maximum coccolithophore depth habitat in this zone is restricted to 60 m. *Emiliania huxleyi* types B/C and C dominate the PFZ and reach relatively high numbers north of the PF, although *E. huxleyi* type O is still present in low abundance (Fig. 11), as also observed by Malinverno et al. (2015). The high coccolithophore numbers observed in the SAZ and at the shallowest depths of the PFZ are part of the Great Calcite Belt, a region of high surface reflectance in the Southern Ocean due to the increased seasonal concentrations of coccolithophore and particulate inorganic carbon (Balch et al., 2011; Balch et al., 2016). We suggest that the uneven distribution of some of the coccolithophore taxa is driven by the physical processes of the ACC; i.e., it is primarily linked to the positions of frontal boundaries but also affected by the dynamics of mesoscale eddies, as mentioned by Holligan et al. (2010).

Minor taxa present in the PFZ, and broadly north of the PF include species of the family Papposphaeraceae (i.e., *Papposphaera* sp., *Pappomonas* spp. and *W. Antarctica*). They have small-sized and lightly calcified coccoliths, which makes them easily overlooked even under SEM. Specimens from the genera *Papposphaera* and *Pappomonas* have been observed at polar waters in the North Hemisphere (Thomsen, 1981; Samtleben and Schröder, 1992; Charalampopoulou et al., 2011; Thomsen and Østergaard, 2014) and also in the Southern Ocean (e.g., Gravalosa et al., 2008; Saavedra-Pellitero et al., 2014; Charalampopoulou et al., 2016). Apart from the fact that the lightly calcified polar coccolithophores are non-photosynthetic heterotrophs, which gives them a strong competitive advantage to dwell in the darkness for months every year, very little is known about them (Thomsen and Østergaard, 2013). However, because they are weakly calcified, they will be one of the first polar taxa to be threatened by ocean acidification (Thomsen and Østergaard, 2013).

#### **4.3. *Emiliania huxleyi* mass variations across the Drake Passage.**

In this study, the coccolith mass of *E. huxleyi* was measured across the Drake Passage up to the PF at depths ranging between 10 and 20 m water depth. The general southwards decreasing trend in *E. huxleyi* mass (Fig. 11) is in agreement with trends observed by Charalampopoulou et al. (2016) across the Southern Ocean (Fig. 13). Differences in the estimated masses can be attributed to the distinct taxonomical considerations, to the methodologies used in both studies, and mainly to the different oceanographic conditions during the sampling periods (2009, 2016). The mean coccolith mass is related to strong latitudinal gradients in temperature ( $r=0.75$ ), also observed by Charalampopoulou et al. (2016), total alkalinity ( $r=-0.89$ ), total  $\text{CO}_2$  ( $r=-0.86$ ),  $\text{HCO}_3^-$  ( $r=-0.81$  or  $-0.68$  depending on the method used to calculate it) in agreement with Beaufort et al., (2011) and nutrient content (nitrate:  $r=-0.75$ , phosphate  $=-0.71$ ) noted by Charalampopoulou et al., (2016) (Table 4, Fig. 12). In contrast, the coccolith mass relationship to salinity, fluorescence, silicate content, carbonate ion, calcite saturation is not significant (Table 4). Still it could be argued that the poleward decrease in coccolith mass roughly coincides with a reduction in  $\Omega_{\text{Ca}}$  (Fig. 12) and  $\text{CO}_3^{2-}$  (Table 4) in agreement with different studies that found depressed coccolith calcification at low  $\Omega_{\text{Ca}}$  and  $\text{CO}_3^{2-}$  values (e.g., Riebesell et al., 2000; Beaufort et al., 2011). Although the pH variation is rather reduced, the anticorrelation between coccolith mass and pH becomes significant ( $r=-0.7$ ) depending on the method used (Table 4, Fig. 12), in agreement with the biogeochemistry and optics South Pacific experiment (BIOSOPE) data from Beaufort et al (2011) ( $r=-0.52$ ). The negative correlation of the present data contrasts with the global and well established relationship between coccolith mass and pH ( $r=0.75$ ) (Beaufort et al., 2011). However, the relationship between coccolith mass and the carbonate chemistry parameters should be considered carefully.  $T_{\text{ALK}}$ ,  $T_{\text{CO}_2}$ ,  $\Omega_{\text{Ca}}$ , pH and  $\text{HCO}_3^-$  have been calculated from the GLODAP-v2 database (in which the majority of the datapoints are scattered and samples were measured just in August 2005 and in February 2009) (Key et al., 2015) or from the global alkalinity and total dissolved carbon collection (Goyet et al., 2000) which shows an austral summer average using the CO2SYS.XLS program (Pierrot et al., 2006).

The observed decreasing trend of the coccolith mass can be linked to the latitudinal succession from type A group to type B group (Fig 12 b), in agreement with other authors who observed a latitudinal trend from *E. huxleyi* more calcified to weakly calcified morphotypes (e.g., Cubillos et al., 2007; Mohan et al., 2008). In the Chilean margin, the highest coccolith masses recorded are related to the presence of *E. huxleyi* type A (including normal, calcified and overcalcified specimens) and type R (Fig. 11), observed also by other authors at lower latitudes offshore Chile (Beaufort et al., 2008; Beaufort et al., 2011; von Dassow et al., 2018). Although it is uncommon, heavily calcified *E. huxleyi* morphotypes have been recorded in reduced pH and  $\Omega_{\text{Ca}}$  conditions in other

parts of the globe (e.g., Smith et al., 2012; Triantaphyllou et al., 2018). The presence of calcified specimens of *E. huxleyi* type B/C, and in a lesser extent of type C, in the transitional zone from the chilean margin to the open ocean reflects an increase in the coccolith masses (Figs. 10, 11). In contrast, a higher relative abundance of *E. huxleyi* type C correponds to smaller coccolith masses in the SAZ. Striking are the relatively low coccolith mass values in the open ocean of the SAZ that coincide with maxima in the density of coccolithophores (Fig. 12).

The dataset presented here constitutes an important contribution to the coccolithophore ecology sparsely studied at high latitudes. This work is also relevant for future climate and ocean model simulations in the context of global warming and ocean acidification threatening calcifying plankton. Taking into account the existing relationships between the physico-chemical parameters and the 10 coccolithophore components, changes in the composition and calcification modes of *E. huxleyi* morphotypes are expected to occur in the Drake Passage with the ongoing climate change. However, our study does not provide enough evidence to infer how coccolithophores will cope with a forthcoming changing ocean. We speculate that future sea surface warming and stratification (Boyd et al., 2008), concomitant with a southward migration of the Antarctic Circumpolar fronts, will lead to a increase in the 15 numbers of *E. huxleyi* at higher latitudes and to a potential higher calcification poleward in agreement with the model from Krumhardt et al. (2017). At the same time, pH,  $\text{CO}_3^{2-}$  and  $\Omega_{\text{Ca}}$  are predicted to decrease (e.g., Hauri et al., 2015), which will also affect coccolithophores. Based on our limited data, conflicting conclusions can be drawn from the carbonate parameters. We could 20 hypothesize that *E. huxleyi* will calcify more in a future Southern Ocean scenario at lower pH, consistent with few culture experiments (e.g., Iglesias-Rodriguez et al., 2008) but also that this species will reduce its calcification rate at lower  $\text{CO}_3^{2-}$ ,  $\Omega_{\text{Ca}}$  and higher  $\text{HCO}_3^-$ , in agreement with the negative effects of ocean acidification suggested by several authors (e.g., Riebesell et al., 2000). Bearing in mind that culture experiments in different strains of *E. huxleyi* have already shown different responses to changing carbonate chemistry (Langer et al., 2009), it seems necessary to consider also the degree of adaptive potential of coccolithophores in future studies to predict their upcoming performance in the Polar realm.

## 5. Conclusions

25 This study documents the latitudinal and the depth variability in the coccolithophore assemblage composition and calcification of *Emiliania huxleyi*, the dominant species, across the Drake Passage, driven by physical, chemical and biological parameters in the surface ocean. Coccolithophore abundance, diversity and maximum depth habitat decrease southwards portraying the oceanographic fronts as ecological boundaries. Marked shifts in the coccolithophore numbers, community composition and diversity occur at the Subantarctic Front (SAF) and Polar Front (PF). Three main different oceanographic areas are characterized, 30 based on the coccolithophore composition:

- (1) The Chilean margin. *Emiliania huxleyi* type A (normal and overcalcified) and type R are present in the stations closest to the Chilean coast, which record the highest SST and lowest SSS in the study area. Rare taxa present offshore Chile are *Calcidiscus* s.l., *Ophiaster* spp. and *Gephyrocapsa muellerae*.
- (2) The Subantarctic Zone (SAZ). This zone is bounded by the SAF in the south. Salinity values are relatively constant and SST gradually decreases while nutrient content increases. The SAZ is characterized by the dominance of *E. huxleyi* types C, B/C, O and B. *Emiliania huxleyi* reaches maximum values of  $212.5 \times 10^3$  cells/L north in the SAZ. Minor taxa include *Syracosphaera* spp. (including holococcolithophores from this genus), *Calcidiscus* sp. and *Acanthoica quattrospina*.

(3) The Polar Front Zone (PFZ). It is bounded by the SAF in the north and the PF in the south. Salinity and SST progressively decreases with respect to the SAZ, and nutrient contents continue to increase poleward. *Emiliania huxleyi* types B/C and C dominate the PFZ and reach relatively high numbers north of the PF, although *E. huxleyi* type O is still present. Minor taxa present in the PFZ, and broadly north of the PF include species of the family Papposphaeraceae (i.e., *Papposphaera* sp, *Pappomonas* spp. 5 and *Wigwamma antarctica*). Specimens of *E. huxleyi* and *W. antarctica* are sporadically recorded south of the PF with numbers of <3\*10<sup>3</sup>cell/L and dwelling a at temperatures <2° C.

The general decreasing trend in *E. huxleyi* coccolith mass can be linked to the latitudinal succession from type A group (in the Chilean margin) to type B group (in the PFZ). Coccolith mass and coccolithophore diversity are related to the strong latitudinal 10 gradient in temperature. Coccolith mass also shows anticorrelation to total alkalinity, total CO<sub>2</sub>, bicarbonate ion (HCO<sub>3</sub><sup>-</sup>), pH and nutrient content, which contrasts with the global and well established positive relationship between coccolith mass and pH as well as total alkalinity. However, the relationship between coccolith mass and the carbonate chemistry parameters should be considered carefully, since in situ measurements are not available. The existing relationships between the physico-chemical parameters and the coccolithophore components in the Drake Passage suggest that assemblage composition and calcification modes of *E. huxleyi* 15 will be strongly affected by the ongoing climate change.

## 6. Acknowledgements

20 The Alfred-Wegener-Institute Bremerhaven provided the plankton samples required for this study. R/V POLARSTERN officers and crew are thanked for their help during PS97 Expedition. Marius Becker (University of Kiel) is acknowledged for his help with MATLAB<sup>TM</sup>, Jeremy Young (University College London) for his assistance with coccolithophore identification and Chloe Anderson (Marum) as well as Diederik Liebrand (University of Bremen) for their comments on the manuscript. Funding was provided by the Deutsche Forschungsgemeinschaft (DFG), Reference: BA 1648/30-1, to M. Saavedra-Pellitero.

25 Data is available in the Pangaea data repository: <https://doi.org/10.1594/PANGAEA.901294>.

## 7. References

5 Balch, W. M., Drapeau, D. T., Bowler, B. C., Lyczkowski, E., Booth, E. S., and Alley, D.: The contribution of coccolithophores to the optical and inorganic carbon budgets during the Southern Ocean Gas Exchange Experiment: New evidence in support of the “Great Calcite Belt” hypothesis, *Journal of Geophysical Research: Oceans*, 116, <http://dx.doi.org/10.1029/2011JC006941>, 2011.

10 Balch, W. M., Bates, N. R., Lam, P. J., Twining, B. S., Rosengard, S. Z., Bowler, B. C., Drapeau, D. T., Garley, R., Lubelczyk, L. C., Mitchell, C., and Rauschenberg, S.: Factors regulating the Great Calcite Belt in the Southern Ocean and its biogeochemical significance, *Global Biogeochemical Cycles*, 30, 1124-1144, <http://doi.org/10.1002/2016gb005414>, 2016.

15 Beaufort, L., Couapel, M., Buchet, N., Claustre, H., and Goyet, C.: Calcite production by coccolithophores in the south east Pacific Ocean, *Biogeosciences*, 5, 1101-1117, <http://doi.org/10.5194/bg-5-1101-2008>, 2008.

20 Beaufort, L., Probert, I., de Garidel-Thoron, T., Bendif, E. M., Ruiz-Pino, D., Metzl, N., Goyet, C., Buchet, N., Coupel, P., Grelaud, M., Rost, B., Rickaby, R. E. M., and de Vargas, C.: Sensitivity of coccolithophores to carbonate chemistry and ocean acidification, *Nature*, 476, 80-83, <http://doi.org/10.1038/nature10295>, 2011.

25 Blanco-Ameijeiras, S., Lebrato, M., Stoll, H. M., Iglesias-Rodriguez, D., Müller, M. N., Méndez-Vicente, A., and Oschlies, A.: Phenotypic Variability in the Coccolithophore *Emiliania huxleyi*, *PLoS one*, 11, e0157697-e0157697, <http://doi.org/10.1371/journal.pone.0157697>, 2016.

30 Boyd, P. W., Doney, S. C., Strzepek, R., Dusenberry, J., Lindsay, K., and Fung, I.: Climate-mediated changes to mixed-layer properties in the Southern Ocean: assessing the phytoplankton response, *Biogeosciences*, 5, 847-864, <https://doi.org/10.5194/bg-5-847-2008>, 2008.

35 Cabré, A., Marinov, I., and Leung, S.: Consistent global responses of marine ecosystems to future climate change across the IPCC AR5 earth system models, *Climate Dynamics*, 45, 1253-1280, <http://doi.org/10.1007/s00382-014-2374-3>, 2015.

40 Cárdenas, P., Lange, C. B., Vernet, M., Esper, O., Srain, B., Vorrath, M.-E., Ehrhardt, S., Müller, J., Kuhn, G., Arz, H. W., Lembke-Jene, L., and Lamy, F.: Biogeochemical proxies and diatoms in surface sediments across the Drake Passage reflect oceanic domains and frontal systems in the region, *Progress in Oceanography*, <https://doi.org/10.1016/j.pocean.2018.10.004>, 2018.

45 Charalampopoulou, A., Poulton, A. J., Tyrrell, T., and Lucas, M. I.: Irradiance and pH affect coccolithophore community composition on a transect between the North Sea and the Arctic Ocean, *Marine Ecology Progress Series*, 431, 25-43, <http://doi.org/10.3354/meps09140>, 2011.

50 Charalampopoulou, A., Poulton, A. J., Bakker, D. C. E., Lucas, M. I., Stinchcombe, M. C., and Tyrrell, T.: Environmental drivers of coccolithophore abundance and calcification across Drake Passage (Southern Ocean), *Biogeosciences*, 13, 5917-5935, <http://doi.org/10.5194/bg-13-5917-2016>, 2016.

55 Comiso, J. C.: Large-scale Characteristics and Variability of the Global Sea Ice Cover, in: *Sea Ice*, 2003.

5 Cook, S. S., Whittock, L., Wright, S. W., and Hallegraeff, G. M.: Photosynthetic pigment and genetic differences between two Southern Ocean morphotypes of *Emiliania huxleyi* (Haptophyta), *Journal of Phycology*, 47, 615-626, <http://doi.org/10.1111/j.1529-8817.2011.00992.x>, 2011.

60 Cubillos, J. C., Wright, S. W., Nash, G., de Salas, M. F., Griffiths, B., Tilbrook, B., Poisson, A., and Hallegraeff, G. M.: Calcification morphotypes of the coccolithophorid *Emiliania huxleyi* in the Southern Ocean: changes in 2001 to 2006 compared to historical data, *Marine Ecology Progress Series*, 348, 47-54, <http://doi.org/10.3354/meps07058>, 2007.

65 Davis, J. C.: *Statistics and Data Analysis in Geology*, 1986.

70 Dylmer, C. V., Giraudeau, J., Hanquiez, V., and Husum, K.: The coccolithophores *Emiliania huxleyi* and *Coccolithus pelagicus*: Extant populations from the Norwegian-Iceland Sea and Fram Strait, *Deep-Sea Research I: Oceanographic Research Papers*, 98, 1-9, <https://doi.org/10.1016/j.dsr.2014.11.012>, 2015.

75 Eynaud, F., Giraudeau, J., Pichon, J. J., and Pudsey, C. J.: Sea-surface distribution of coccolithophores, diatoms, silicoflagellates and dinoflagellates in the South Atlantic Ocean during the late austral summer 1995, *Deep Sea Research Part I: Oceanographic Research Papers*, 46, 451-482, [https://doi.org/10.1016/S0967-0637\(98\)00079-X](https://doi.org/10.1016/S0967-0637(98)00079-X), 1999.

80 Fabry, V. J., Seibel, B. A., Feely, R. A., and Orr, J. C.: Impacts of ocean acidification on marine fauna and ecosystem processes, *ICES Journal of Marine Science*, 65, 414-432, <https://doi.org/10.1093/icesjms/fsn048>, 2008.

85 Fabry, V. J., McClintock, J. B., Mathis, J. T., and Grebmeier, J. M.: Ocean acidification at high latitudes: The bellwether, *Oceanography*, 22, 160-171, <https://doi.org/10.5670/oceanog.2009.105>, 2009.

90 Findlay, C. S., and Giraudeau, J.: Extant calcareous nannoplankton in the Australian Sector of the Southern Ocean (austral summers 1994 and 1995), *Marine Micropaleontology*, 40, 417-439, [https://doi.org/10.1016/S0377-8398\(00\)00046-3](https://doi.org/10.1016/S0377-8398(00)00046-3), 2000.

95 Findlay, H. S., Calosi, P., and Crawfurd, K.: Determinants of the PIC : POC response in the coccolithophore *Emiliania huxleyi* under future ocean acidification scenarios, *Limnology and Oceanography*, 56, 1168-1178, <https://doi.org/10.4319/lo.2011.56.3.1168>, 2011.

Franks, P. J. S.: Sink or swim: accumulation of biomass at fronts, *Marine Ecology-Progress Series*, 82, 1-12, <https://doi.org/10.3354/meps082001>, 1992.

Freeman, N. M., and Lovenduski, N. S.: Decreased calcification in the Southern Ocean over the satellite record, *Geophysical Research Letters*, 42, 1834–1840, <https://doi.org/10.1002/2014gl062769>, 2015.

5 Frenger, I., Münnich, M., and Gruber, N.: Imprint of Southern Ocean mesoscale eddies on chlorophyll, *Biogeosciences*, 15, 4781-4798, <https://doi.org/10.5194/bg-15-4781-2018>, 2018.

Fuertes, M.-Á., Flores, J.-A., and Sierro, F. J.: The use of circularly polarized light for biometry, identification and estimation of mass of coccoliths, *Marine Micropaleontology*, 113, 44-55, <https://doi.org/10.1016/j.marmicro.2014.08.007>, 2014.

10 Garcia, H. E., Locarnini, R. A., Boyer, T. P., Antonov, J. I., Baranova, O. K., Zweng, M. M., Reagan, J. R., and Johnson, D. R.: World Ocean Atlas 2013, in: NOAA Atlas NESDIS 76, edited by: Levitus, S. E., A. Mishonov Technical Ed., U.S. Government Printing Office, Washington, D.C., 25, 2014.

Gattuso, J.-P., Bijma, J., Gehlen, M., Riebesell, U., and Turley, C.: Ocean acidification: knowns, unknowns and perspectives, in: Ocean acidification, edited by: Gattuso, J.-P., and Hansson, L., Oxford University Press, Oxford, 291-311, 2011.

15 Giraudeau, J., Bailey, G. W., and Pujol, C.: A high-resolution time-series analyses of particle fluxes in the Northern Benguela coastal upwelling system: carbonate record of changes in biogenic production and particle transfer processes, *Deep Sea Research Part II: Topical Studies in Oceanography*, 47, 1999-2028, [https://doi.org/10.1016/S0967-0645\(00\)00014-X](https://doi.org/10.1016/S0967-0645(00)00014-X), 2000.

Giraudeau, J., Hulot, V., Hanquiez, V., Devaux, L., Howa, H., and Garlan, T.: A survey of the summer coccolithophore community in the western Barents Sea, *Journal of Marine Systems*, 158, 93-105, <https://doi.org/10.1016/j.jmarsys.2016.02.012>, 2016.

20 Gravalosa, J. M., Flores, J.-A., Sierro, F. J., and Gersonde, R.: Sea surface distribution of coccolithophores in the eastern Pacific sector of the Southern Ocean (Bellingshausen and Amundsen Seas) during the late austral summer of 2001, *Marine Micropaleontology*, 69, 16-25, <https://doi.org/10.1016/j.marmicro.2007.11.006>, 2008.

Hagino, K., Okada, H., and Matsuoka, H.: Coccolithophore assemblages and morphotypes of *Emiliania huxleyi* in the boundary zone between the cold Oyashio and warm Kuroshio currents off the coast of Japan, *Marine Micropaleontology*, 55, 19-47, <https://doi.org/10.1016/j.marmicro.2005.02.002>, 2005.

25 Hagino, K., Bendif, E. M., Young, J. R., Kogame, K., Probert, I., Takano, Y., Horiguchi, T., de Vargas, C., and Okada, H.: New evidence for morphological and genetic variation in the cosmopolitan coccolithophore *Emiliania huxleyi* (Prymnesiophyceae) from the COX1b-ATP4 genes, *Journal of Phycology*, 47, 1164-1176, <https://doi.org/10.1111/j.1529-8817.2011.01053.x>, 2011.

30 Hammer, Ø., Harper, D. A. T., and Ryan, P. D.: PAST: paleontological Statistics software package for education and data analysis, *Paleontologia Electronica*, 49, 9, [http://palaeo-electronica.org/2001\\_1/past/issue1\\_01.htm](http://palaeo-electronica.org/2001_1/past/issue1_01.htm), 2001.

Harada, N., Sato, M., Oguri, K., Hagino, K., Okazaki, Y., Katsuki, K., Tsuji, Y., Shin, K.-H., Tadai, O., Saitoh, S.-I., Narita, H., Konno, S., Jordan, R. W., Shiraiwa, Y., and Grebmeier, J.: Enhancement of coccolithophorid blooms in the Bering Sea by recent environmental changes, *Global Biogeochemical Cycles*, 26, GB2036, <https://doi.org/10.1029/2011gb004177>, 2012.

35 Harper, D. A. T.: *Numerical Palaeobiology*, John Wiley & Sons, 1999.

Hauri, C., Friedrich, T., and Timmermann, A.: Abrupt onset and prolongation of aragonite undersaturation events in the Southern Ocean, *Nature Climate Change*, 6, 172, <https://doi.org/10.1038/nclimate2844>, 2015.

Hinz, D. J., Poulton, A. J., NIELSDÓTTIR, M. C., Steigenberger, S., Korb, R. E., Achterberg, E. P., and Bibby, T. S.: Comparative seasonal biogeography of mineralising nannoplankton in the Scotia Sea: *Emiliania huxleyi*, *Fragilariopsis* spp. and *Tetraparma pelagica*, *Deep Sea Research Part II: Topical Studies in Oceanography*, 59-60, 57-66, <https://doi.org/10.1016/j.dsr2.2011.09.002>, 2012.

40 Hiramatsu, C., and De Deckker, P.: Distribution of calcareous nannoplankton near the Subtropical Convergence, south of Tasmania, Australia, *Marine and Freshwater Research*, 47, 707-713, <https://doi.org/10.1071/MF9960707>, 1996.

Holligan, P. M., Fernández, E., Aiken, J., Balch, W. M., Boyd, P., Burkhill, P. H., Finch, M., Groom, S. B., Malin, G., Muller, K., Purdie, D. A., Robinson, C., Trees, C. C., Turner, S. M., and van der Wal, P.: A biogeochemical study of the coccolithophore, *Emiliania huxleyi*, in the North Atlantic, *Global Biogeochemical Cycles*, 7, 879-900, <https://doi.org/10.1029/93gb01731>, 1993.

45 Holligan, P. M., Charalampopoulou, A., and Hutson, R.: Seasonal distributions of the coccolithophore, *Emiliania huxleyi*, and of particulate inorganic carbon in surface waters of the Scotia Sea, *Journal of Marine Systems*, 82, 195-205, <https://doi.org/10.1016/j.jmarsys.2010.05.007>, 2010.

50 Iglesias-Rodriguez, M. D., Halloran, P. R., Rickaby, R. E. M., Hall, I. R., Colmenero-Hidalgo, E., Gittins, J. R., Green, D. R. H., Tyrrell, T., Gibbs, S. J., von Dassow, P., Rehm, E., Armbrust, E. V., and Boessenkool, K. P.: Phytoplankton calcification in a high-CO<sub>2</sub> world, *Science*, 320, 336-340, 10.1126/science.1154122, 2008.

Iglesias-Rodriguez, M. D., Jones, B. M., Blanco-Ameijeiras, S., Greaves, M., Huete-Ortega, M., and Lebrato, M.: Physiological responses of coccolithophores to abrupt exposure of naturally low pH deep seawater, *PLOS ONE*, 12, e0181713, <https://doi.org/10.1371/journal.pone.0181713>, 2017.

55 Jordan, R. W., Cros, L., and Young, J. R.: A revised classification scheme for living haptophytes, *Micropaleontology*, 50, 55-79, [https://doi.org/10.2113/50.Suppl\\_1.55](https://doi.org/10.2113/50.Suppl_1.55), 2004.

Key, R. M., Olsen, A., van Heuven, S., Lauvset, S. K., Velo, A., Lin, X., Schirnick, C., Kozyr, A., Tanhua, T., Hoppema, M., Jutterström, S., Steinfeldt, R., Jeansson, E., Ishii, M., Perez, F. F., and Suzuki, T.: Global Data Analysis Project (GLODAP), Version 2, 2015.

Krumhardt, K. M., Lovenduski, N. S., Freeman, N. M., and Bates, N. R.: Apparent increase in coccolithophore abundance in the subtropical North Atlantic from 1990 to 2014, *Biogeosciences*, 13, 1163-1177, 10.5194/bg-13-1163-2016, 2016.

Krumhardt, K. M., Lovenduski, N. S., Iglesias-Rodriguez, M. D., and Kleypas, J. A.: Coccolithophore growth and calcification in a changing ocean, *Progress in Oceanography*, 159, 276-295, <https://doi.org/10.1016/j.pocean.2017.10.007>, 2017.

Krumhardt, K. M., Lovenduski, N. S., Long, M. C., Levy, M., Lindsay, K., Moore, J. K., and Nissen, C.: Coccolithophore growth and calcification in an acidified ocean: Insights from Community Earth System Model simulations, *Journal of Advances in Modeling Earth Systems*, <https://doi.org/10.1029/2018ms001483>, 2019.

Lamy, F.: The Expedition PS97 of the Research Vessel POLARSTERN to the Drake Passage in 2016, edited by: Lamy, F, *Berichte zur Polar- und Meeresforschung, Reports on Polar and Marine Research*, 167 pp., [http://doi.org/10.2312/BzPM\\_0701\\_2016](http://doi.org/10.2312/BzPM_0701_2016), 2016.

Langer, G., Nehrke, G., Probert, I., Ly, J., and Ziveri, P.: Strain-specific responses of *Emiliania huxleyi* to changing seawater carbonate chemistry, *Biogeosciences*, 6, 2637-2646, <https://doi.org/10.5194/bg-6-2637-2009>, 2009.

Laubscher, R. K., Perissinotto, R., and McQuaid, C. D.: Phytoplankton production and biomass at frontal zones in the Atlantic sector of the Southern Ocean, *Polar Biology*, 13, 471-481, <https://doi.org/10.1007/BF00233138>, 1993.

Locarnini, R. A., Mishonov, A. V., Antonov, J. I., Boyer, T. P., Garcia, H. E., Baranova, O. K., Zweng, M. M., Paver, C. R., Reagan, J. R., Johnson, D. R., Hamilton, M., and Seidov, D.: World ocean atlas 2013, in: Volume 1: Temperature, NOAA Atlas NESDIS, vol. 73, edited by: Levitus, S. A. E., Mishonov Technical Ed., NOAA, Silver Spring, Md, 40, 2013.

Malinverno, E., Triantaphyllou, M. V., and Dimiza, M. D.: Coccolithophore assemblage distribution along a temperate to polar gradient in the West Pacific sector of the Southern Ocean (January 2005), *Micropaleontology*, 61, 489-506 2015.

Malinverno, E., Maffioli, P., and Gariboldi, K.: Latitudinal distribution of extant fossilizable phytoplankton in the Southern Ocean: Planktonic provinces, hydrographic fronts and palaeoecological perspectives, *Marine Micropaleontology*, 123, 41-58, <https://doi.org/10.1016/j.marmicro.2016.01.001>, 2016.

Malone, T., Azzaro, M., Bode, A., Brown, E., Duce, R., Kamykowski, D., Kang, S. H., Kedong, Y., Thorndyke, M., Wang, J., Park, C., Calumpong, H., and Egertson, P.: Primary Production, Cycling of Nutrients, Surface Layer and Plankton, in: *The First Global Integrated Marine Assessment: World Ocean Assessment I*, edited by: United, N., Cambridge University Press, Cambridge, 119-148, 2017.

McIntyre, A., and Bé, A. W. H.: Modern coccolithophorids of the Atlantic Ocean. Placoliths and Cyrtoliths, *Deep-Sea Research*, 14, 561-597, 1967.

Medlin, L. K., Barker, G. L. A., Campbell, L., Green, J. C., Hayes, P. K., Marie, D., Wrieden, S., and Vaulot, D.: Genetic characterisation of *Emiliania huxleyi* (Haptophyta), *Journal of Marine Systems*, 9, 13-31, [https://doi.org/10.1016/0924-7963\(96\)00013-9](https://doi.org/10.1016/0924-7963(96)00013-9), 1996.

Menschel, E., González, H. E., and Giesecke, R.: Coastal-oceanic distribution gradient of coccolithophores and their role in the carbonate flux of the upwelling system off Concepción, Chile (36°S), *Journal of Plankton Research*, 38, 798-817, <https://doi.org/10.1093/plankt/fbw037>, 2016.

Mix, A. C., Morey, A. E., Pisias, N. G., and Hostetler, S. W.: Foraminiferal faunal estimates of paleotemperature: Circumventing the No-analog problem yields cool Ice Age tropics, *Paleoceanography*, 14, 350-359, <https://doi.org/10.1029/1999PA900012> 1999.

Mohan, R., Mergulhao, L. P., Guptha, M. V. S., Rajakumar, A., Thamban, M., AnilKumar, N., Sudhakar, M., and Ravindra, R.: Ecology of coccolithophores in the Indian sector of the Southern Ocean, *Marine Micropaleontology*, 67, 30-45, <https://doi.org/10.1016/j.marmicro.2007.08.005>, 2008.

Murphy, E. J.: Spatial structure of the Southern Ocean ecosystem: predator-prey linkages in the Southern Ocean food webs, *Journal of Animal Ecology*, 64, 333-347, 1995.

Nishida, S.: Nanoplankton flora in the Southern Ocean, with special reference to siliceous varieties, *Memoirs of the National Institute for Polar Research* 40, 56-68, 1986.

Nissen, C., Vogt, M., Münnich, M., Gruber, N., and Haumann, F. A.: Factors controlling coccolithophore biogeography in the Southern Ocean, *Biogeosciences*, 15, 6997-7024, <https://doi.org/10.5194/bg-15-6997-2018>, 2018.

O'Brien, C. J., Vogt, M., and Gruber, N.: Global coccolithophore diversity: Drivers and future change, *Progress in Oceanography*, 140, 27-42, <https://doi.org/10.1016/j.pocean.2015.10.003>, 2016.

Okada, H., and Honjo, S.: The distribution of oceanic coccolithophorids in the Pacific, *Deep-Sea Research* 20, 355-374, [https://doi.org/10.1016/0011-7471\(73\)90059-4](https://doi.org/10.1016/0011-7471(73)90059-4), 1973.

Orsi, A. H., Whitworth III, T., and Nowlin Jr, W. D.: On the meridional extent and fronts of the Antarctic Circumpolar Current, *Deep Sea Research Part I: Oceanographic Research Papers*, 42, 641-673, [https://doi.org/10.1016/0967-0637\(95\)00021-w](https://doi.org/10.1016/0967-0637(95)00021-w), 1995.

Patil, S., Mohan, R., Shetye, S., and Gazi, S.: Phytoplankton abundance and community structure in the Antarctic polar frontal region during austral summer of 2009, *Chin. J. Ocean. Limnol.*, 31, 21-30, <https://doi.org/10.1007/s00343-013-1309-x>, 2013.

Patil, S. M., Mohan, R., Shetye, S., Gazi, S., and Jafar, S.: Morphological variability of *Emiliania huxleyi* in the Indian sector of the Southern Ocean during the austral summer of 2010, *Marine Micropaleontology*, 107, 44-58, <https://doi.org/10.1016/j.marmicro.2014.01.005>, 2014.

Pierrot, D., Lewis, E., and Wallace, D. W. R.: MS Excel Program Developed for CO<sub>2</sub> System Calculations. ORNL/CDIAC-105a, Carbon Dioxide Information Analysis Center, Oak Ridge National Laboratory, U.S. Department of Energy, Oak Ridge, Tennessee, 2006.

5 Pollard, R. T., Bathmann, U., Dubischar, C., Read, J. F., and Lucas, M.: Zooplankton distribution and behaviour in the Southern Ocean from surveys with a towed Optical Plankton Counter, Deep Sea Research Part II: Topical Studies in Oceanography, 49, 3889-3915, [https://doi.org/10.1016/S0967-0645\(02\)00116-9](https://doi.org/10.1016/S0967-0645(02)00116-9), 2002.

Post, E., Bhatt, U. S., Bitz, C. M., Brodie, J. F., Fulton, T. L., Hebblewhite, M., Kerby, J., Kutz, S. J., Stirling, I., and Walker, D. A.: Ecological Consequences of Sea-Ice Decline, *Science*, 341, 519-524, <https://doi.org/10.1126/science.1235225>, 2013.

10 Poulton, A. J., Painter, S. C., Young, J. R., Bates, N. R., Bowler, B., Drapeau, D., Lyczczkowski, E., and Balch, W. M.: The 2008 *Emiliania huxleyi* bloom along the Patagonian Shelf: Ecology, biogeochemistry, and cellular calcification, *Global Biogeochemical Cycles*, 27, 1023-1033, <https://doi.org/10.1002/2013gb004641>, 2013.

Riebesell, U., Zondervan, I., Rost, B., Tortell, P. D., Zeebe, R. E., and Morel, F. M. M.: Reduced calcification of marine plankton in response to increased atmospheric CO<sub>2</sub>, *Nature*, 407, 364-367, <https://doi.org/10.1038/35030078>, 2000.

15 Rigual Hernández, A. S., Flores, J. A., Sierro, F. J., Fuertes, M. A., Cros, L., and Trull, T. W.: Coccolithophore populations and their contribution to carbonate export during an annual cycle in the Australian sector of the Antarctic zone, *Biogeosciences*, 15, 1843-1862, <https://doi.org/10.5194/bg-15-1843-2018>, 2018.

Rivero-Calle, S., Gnanadesikan, A., Del Castillo, C. E., Balch, W. M., and Guikema, S. D.: Multidecadal increase in North Atlantic coccolithophores and the potential role of rising CO<sub>2</sub>, *Science*, 350, 1533-1537, <https://doi.org/10.1126/science.aaa8026>, 2015.

20 Saavedra-Pellitero, M., Baumann, K.-H., Flores, J.-A., and Gersonde, R.: Biogeographic distribution of living coccolithophores in the Pacific sector of the Southern Ocean, *Marine Micropaleontology*, 109, 1-20, <https://doi.org/10.1016/j.marmicro.2014.03.003>, 2014.

Saavedra-Pellitero, M., and Baumann, K. H.: Comparison of living and surface sediment coccolithophore assemblages in the Pacific sector of the Southern Ocean, *Micropaleontology*, 61, 507-520, 2015.

25 Samtleben, C., and Schröder, A.: Living coccolithophore communities in the Norwegian-Greenland Sea and their record in sediments, *Marine Micropaleontology*, 19, 333-354, [https://doi.org/10.1016/0377-8398\(92\)90037-K](https://doi.org/10.1016/0377-8398(92)90037-K), 1992.

Saruwatari, K., Satoh, M., Harada, N., Suzuki, I., and Shiraiwa, Y.: Change in coccolith size and morphology due to response to temperature and salinity in coccolithophore *Emiliania huxleyi* (Haptophyta) isolated from the Bering and Chukchi seas, *Biogeosciences*, 13, 2743-2755, <https://doi.org/10.5194/bg-13-2743-2016>, 2016.

30 Schlitzer, R.: Ocean Data View. URL: <https://odv.awi.de/>, 2015.

Smith, H. E. K., Tyrrell, T., Charalampopoulou, A., Dumousseaud, C., Legge, O. J., Birchenough, S., Pettit, L. R., Garley, R., Hartman, S. E., Hartman, M. C., Sagoo, N., Daniels, C. J., Achterberg, E. P., and Hydes, D. J.: Predominance of heavily calcified coccolithophores at low CaCO<sub>3</sub> saturation during winter in the Bay of Biscay, *Proceedings of the National Academy of Sciences of the United States of America*, 109, 8845-8849, <https://doi.org/10.1073/pnas.1117508109>, 2012.

35 Supraha, L., Ljubesic, Z., Mihanovic, H., and Henderiks, J.: Observations on the life cycle and ecology of *Acanthoica quattrospina* Lohmann from a Mediterranean estuary, *Journal of Nannoplankton Research*, 34, 49-56, 2014.

Thomsen, H. A.: Identification by electron-microscopy of nanoplanktonic coccolithophorids (Prymnesiophyceae) from West Greenland, including the description of *Papposphaera sarion* sp. nov., *British Phycological Journal*, 16, 77-94, <https://doi.org/10.1080/00071618100650071>, 1981.

40 Thomsen, H. A., and Østergaard, J. B.: Coccolithophorids in Polar Waters: *Wigwamma* spp. Revisited, *Acta Protozoologica* 52, 237-256, <https://doi.org/10.4467/16890027AP.14.022.1997> 2013.

Thomsen, H. A., and Østergaard, J. B.: Coccolithophorids in Polar Waters: *Pappomonas* spp. Revisited, *Acta Protozoologica* 53, 235-256, <https://doi.org/10.4467/16890027AP.14.022.1997> 2014.

45 Triantaphyllou, M. V., Baumann, K.-H., Karatsolis, B.-T., Dimiza, M. D., Psarra, S., Skampa, E., Patoucheas, P., Vollmar, N. M., Koukousioura, O., Katsigera, A., Krasakopoulou, E., and Nomikou, P.: Coccolithophore community response along a natural CO<sub>2</sub> gradient off Methana (SW Saronikos Gulf, Greece, NE Mediterranean), *PLOS ONE*, 13, e0200012, <https://doi.org/10.1371/journal.pone.0200012>, 2018.

50 van Bleijswijk, J., van der Wal, P., Kempers, R., Veldhuis, M., Young, J. R., Muyzer, G., de Vrind-de Jong, E., and Westbroek, P.: Distribution of two types of *Emiliania huxleyi* (Prymnesiophyceae) in the northeast Atlantic region as determined by immunofluorescence and coccolith morphology, *Journal of Phycology*, 27, 566-570, <https://doi.org/10.1111/j.0022-3646.1991.00566.x>, 1991.

Verbeek, J. W.: Recent Calcareous Nannoplankton in the Southernmost Atlantic, *Polarforschung*, 59, 45-60, 1989.

Verbeek, J. W.: Late Quaternary calcareous nannoplankton biostratigraphy for the northern Atlantic Ocean, *Mededelingen Rijks Geologische Dienst*, 44, 13-33, 1990.

55 von Dassow, P., Díaz-Rosas, F., Bendif, E. M., Gaitán-Espitia, J. D., Mella-Flores, D., Rokitta, S., John, U., and Torres, R.: Overcalcified forms of the coccolithophore *Emiliania huxleyi* in high-CO<sub>2</sub> waters are not preadapted to ocean acidification, *Biogeosciences*, 15, 1515-1534, <https://doi.org/10.5194/bg-15-1515-2018>, 2018.

Wassmann, P., Duarte, C. M., Agustí, S., and Sejr, M. K.: Footprints of climate change in the Arctic marine ecosystem, *Global Change Biology*, 17, 1235-1249, <https://doi.org/10.1111/j.1365-2486.2010.02311.x>, 2011.

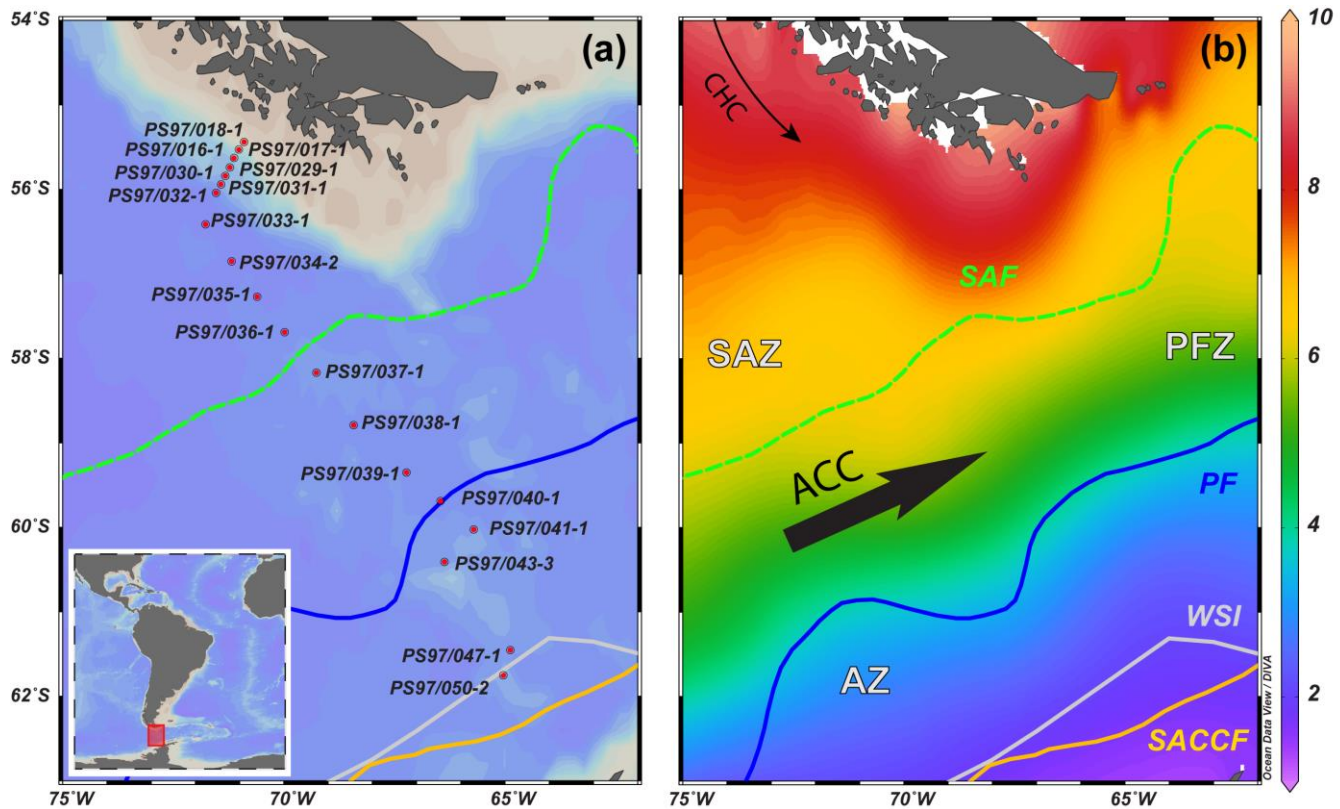
Winter, A., Henderiks, J., Beaufort, L., Rickaby, R. E. M., and Brown, C. W.: Poleward expansion of the coccolithophore *Emiliania huxleyi*, Journal of Plankton Research, 36, 316-325, <https://doi.org/10.1093/plankt/fbt110>, 2014.

Young, J. R., and Westbroek, P.: Genotypic variation in the coccolithophorid species *Emiliania huxleyi*, Marine Micropaleontology, 18, 5-23, [https://doi.org/10.1016/0377-8398\(91\)90004-P](https://doi.org/10.1016/0377-8398(91)90004-P), 1991.

Young, J. R., and Bown, P.: Higher classification of calcareous nannofossils, Journal of Nannoplankton Research, 19, 15-20, 1997.

Young, J. R., Geisen, M., Cros, L., Kleijne, A., Sprengel, C., Probert, I., and Østergaard, J.: A guide to extant coccolithophore taxonomy Journal of Nannoplankton Research, Special Issue 1, 125 pp., 2003.

Young, J. R., Bown P. R., Lees J. A.: Nannotax3 website. International Nannoplankton Association. Accessed April 2019. URL: <http://www.mikrotax.org/Nannotax3>, 2019.



10 **Fig. 1.** (a) Overview map showing the bathymetry of the Drake Passage area and the CTD stations studied; (b) sea surface temperature (°C) seasonal average (January, February, March) at 0 m water depth from the World Ocean Atlas 2013, 0.25° grid (Locarnini et al., 2013) plotted with Ocean Data View (ODV) software version 4.6.3 (Schlitzer, 2015). The different oceanographic fronts are indicated as follows: Subantarctic Front (SAF) with a green dashed line, Antarctic Polar Front (PF) with a blue line and southern Antarctic Circumpolar Current Front (SACCF) with an orange line (Orsi et al., 1995). The areas between the fronts are referred to as Subantarctic Zone (SAZ), Polar Front Zone (PFZ) and Antarctic Zone (AZ). CHC: Cape Horn Current, ACC: Antarctic Circumpolar Current, WSI: winter sea ice extent (Comiso, 2003).

15

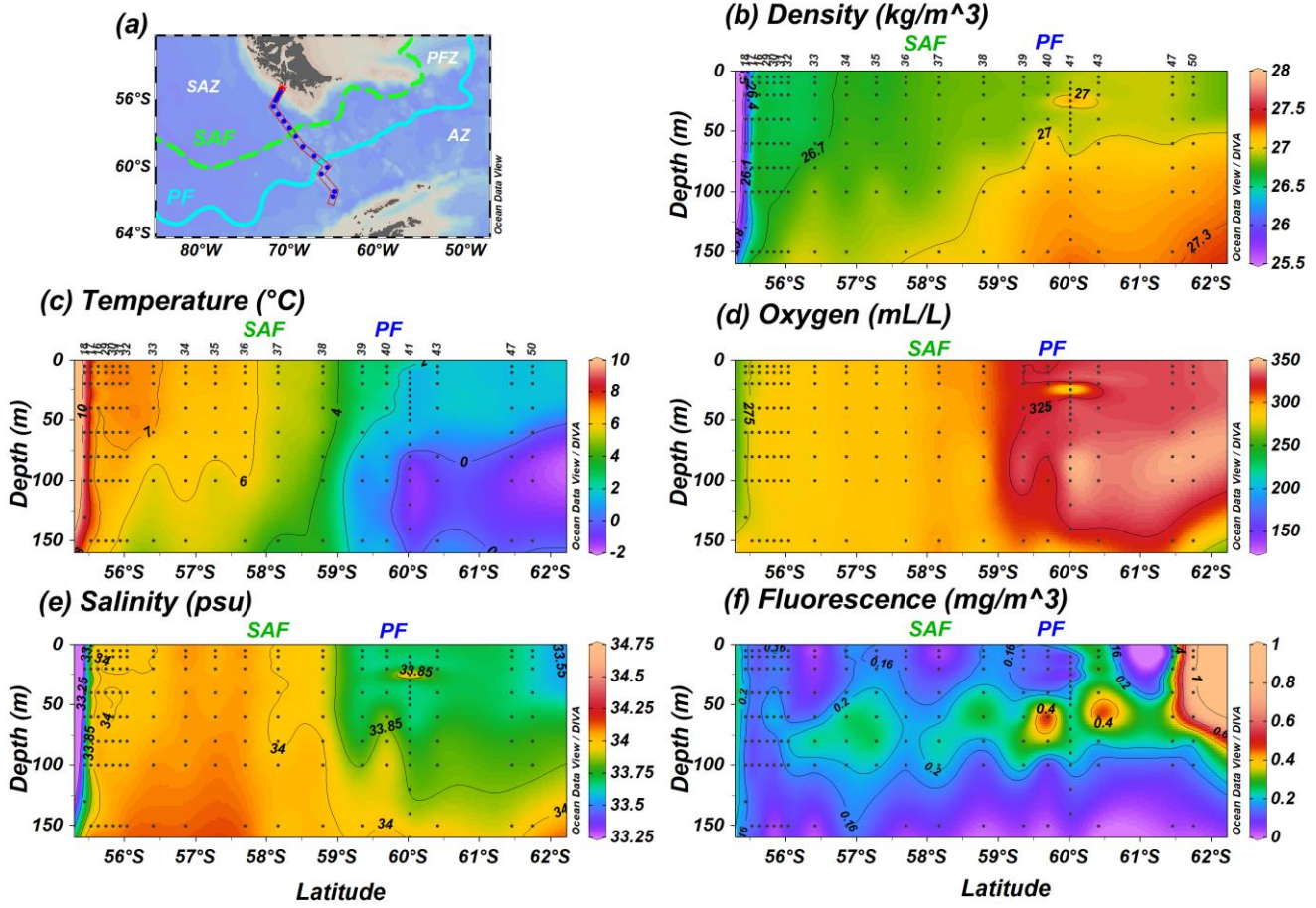


Fig. 2. (a) Location of the PS97 CTD stations studied, (b) water density ( $\text{kg/m}^3$ ), (c) sea surface temperature ( $^{\circ}\text{C}$ ), (d) dissolved oxygen ( $\text{mL/L}$ ) (e) sea surface salinity ( $\text{psu}$ ) and (d) fluorescence ( $\text{mg/m}^3$ ) profiles from  $55.4^{\circ}\text{S}$  to  $61.7^{\circ}\text{S}$  up to a depth of 150 m. Black dots indicate sampling points. The different oceanographic fronts (according to Orsi et al., 1995) are indicated as SAF—green dashed line, PF—blue line.

5

10

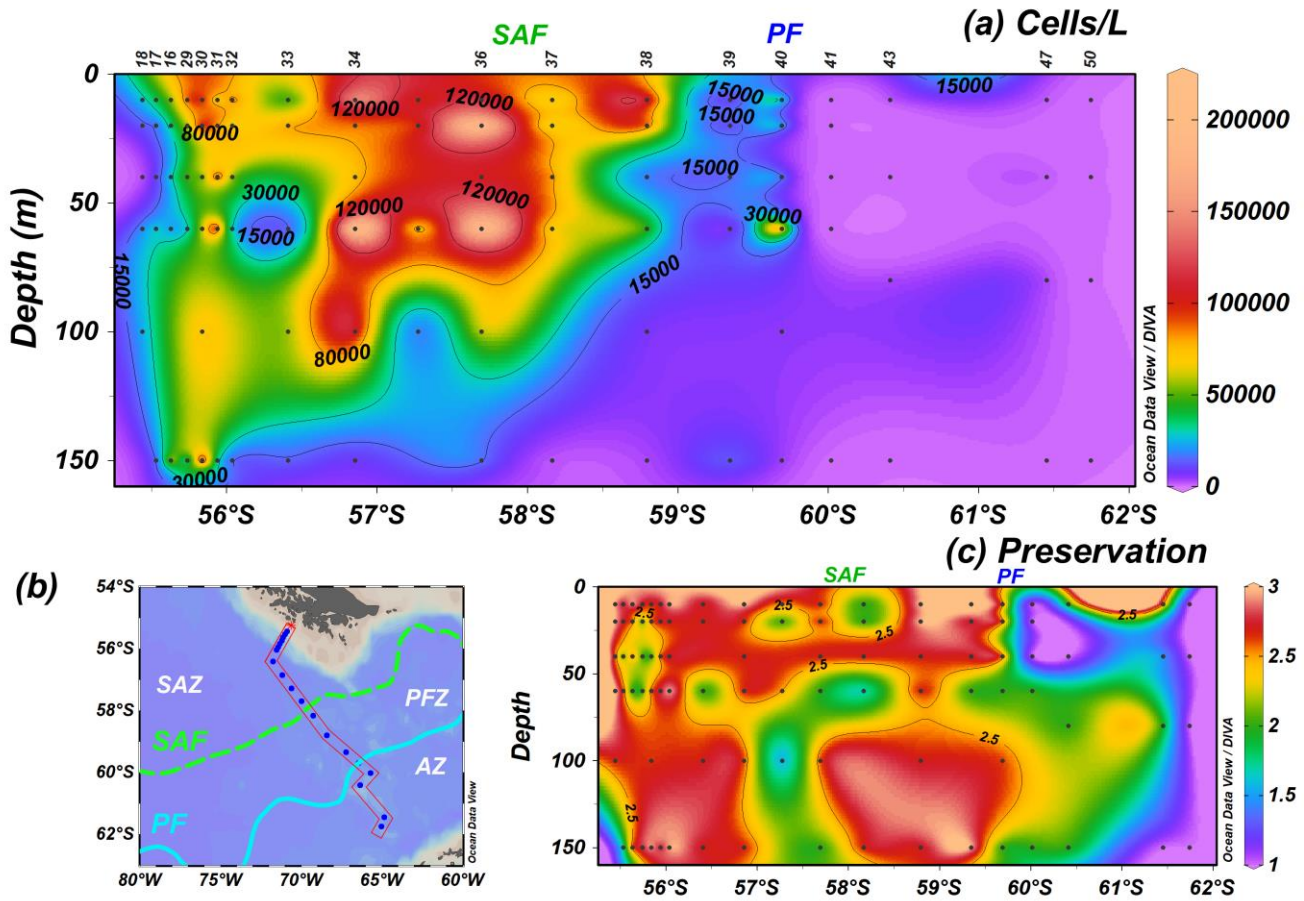
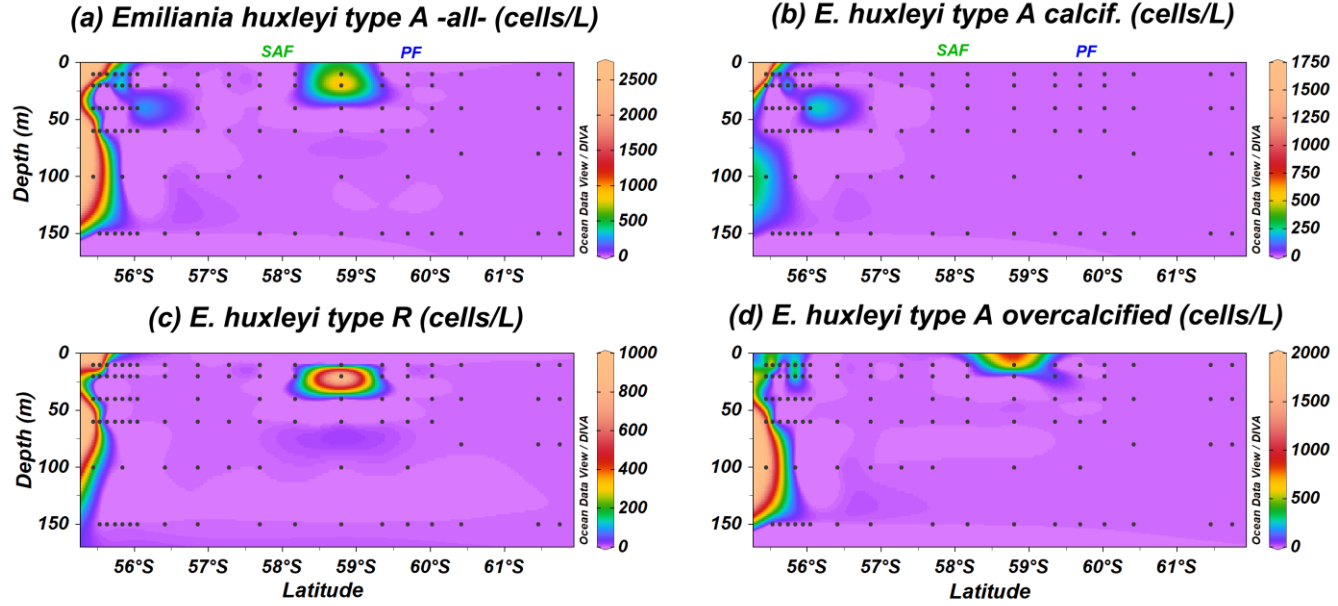


Fig. 3. PS97 CTD stations showing (a) the number of coccospheres/l across a (b) latitudinal transect in the Drake Passage and (c) semiquantitative estimates of coccolith preservation for the uppermost 150 m of the water column (1=poor, 2=moderate, 3=good). Black dots indicate sampling points and the different oceanographic fronts according to Orsi et al., (1995) are indicated as SAF—green dashed line, PF—blue line.



**Fig. 4.** Location of the PS97 CTD stations studied showing the number of coccospores/L of (a) *Emiliania huxleyi* type A group, (b) *E. huxleyi* type A moderately calcified, (c) *E. huxleyi* type R and (d) *E. huxleyi* overcalcified. The Subantarctic Front (SAF) and the Polar Front (PF) according to Orsi et al. (1995) are indicated.

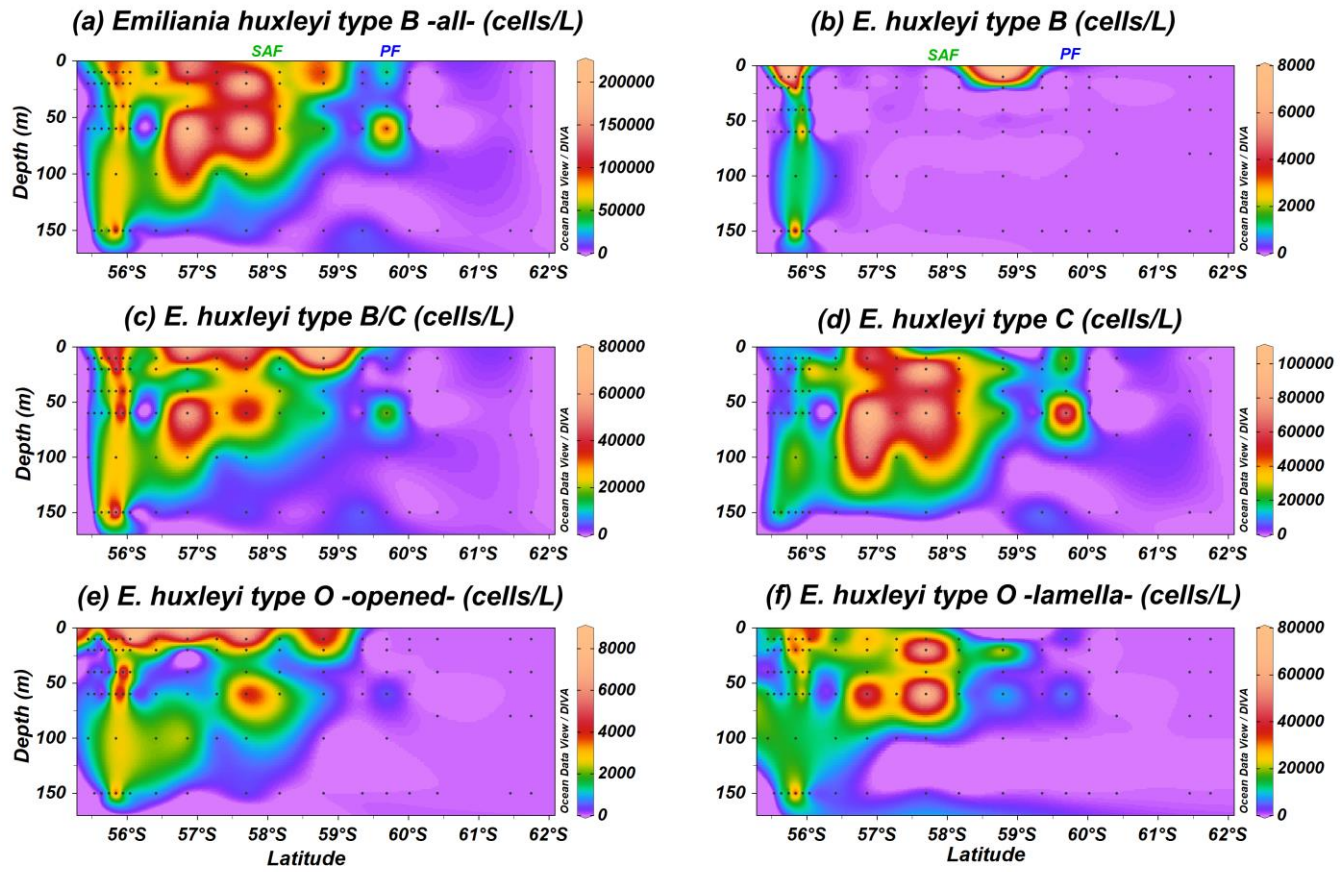


Fig. 5. Location of the PS97 CTD stations studied showing the number of coccospores/L of (a) *Emiliania huxleyi* type B group, (b) *E. huxleyi* type B, (c) *E. huxleyi* type B/C, (d) *E. huxleyi* type C, (e) *E. huxleyi* type O (with opened central area) and (f) *E. huxleyi* type O (with lamella). The Subantarctic Front (SAF) and the Polar Front (PF) according to Orsi et al. (1995) are indicated.

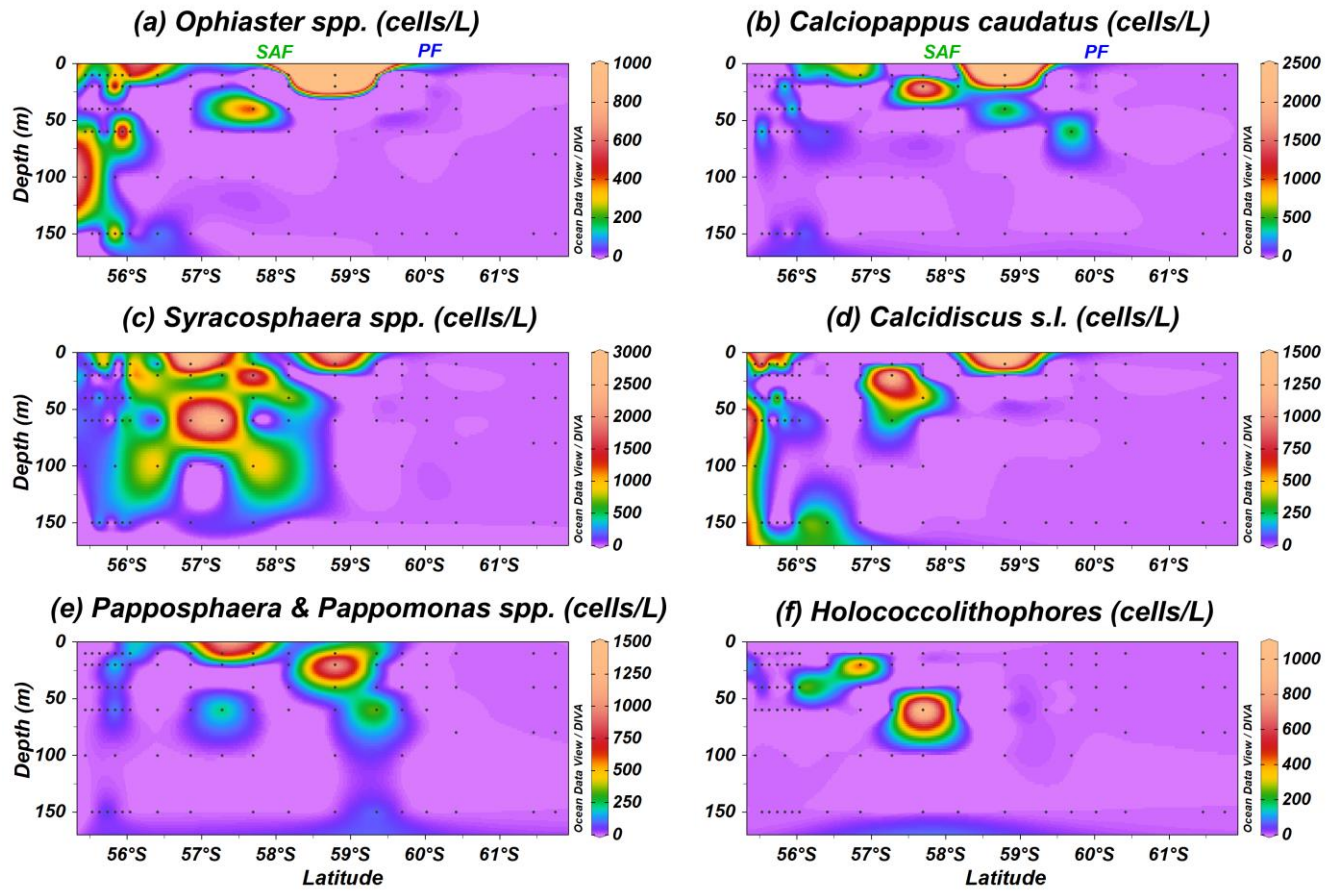


Fig. 6. Location of the PS97 CTD stations studied showing the number of coccospores/L of (a) *Ophiaster spp.*, (b) *Calciopappus caudatus*, (c) *Syracosphaera spp.*, (d) *Calcidiscus s.l.*, (e) *Papposphaera & Pappomonas spp.*, and (f) holocololithophores. The Subantarctic Front (SAF) and the Polar Front (PF) according to Orsi et al. (1995) are indicated.

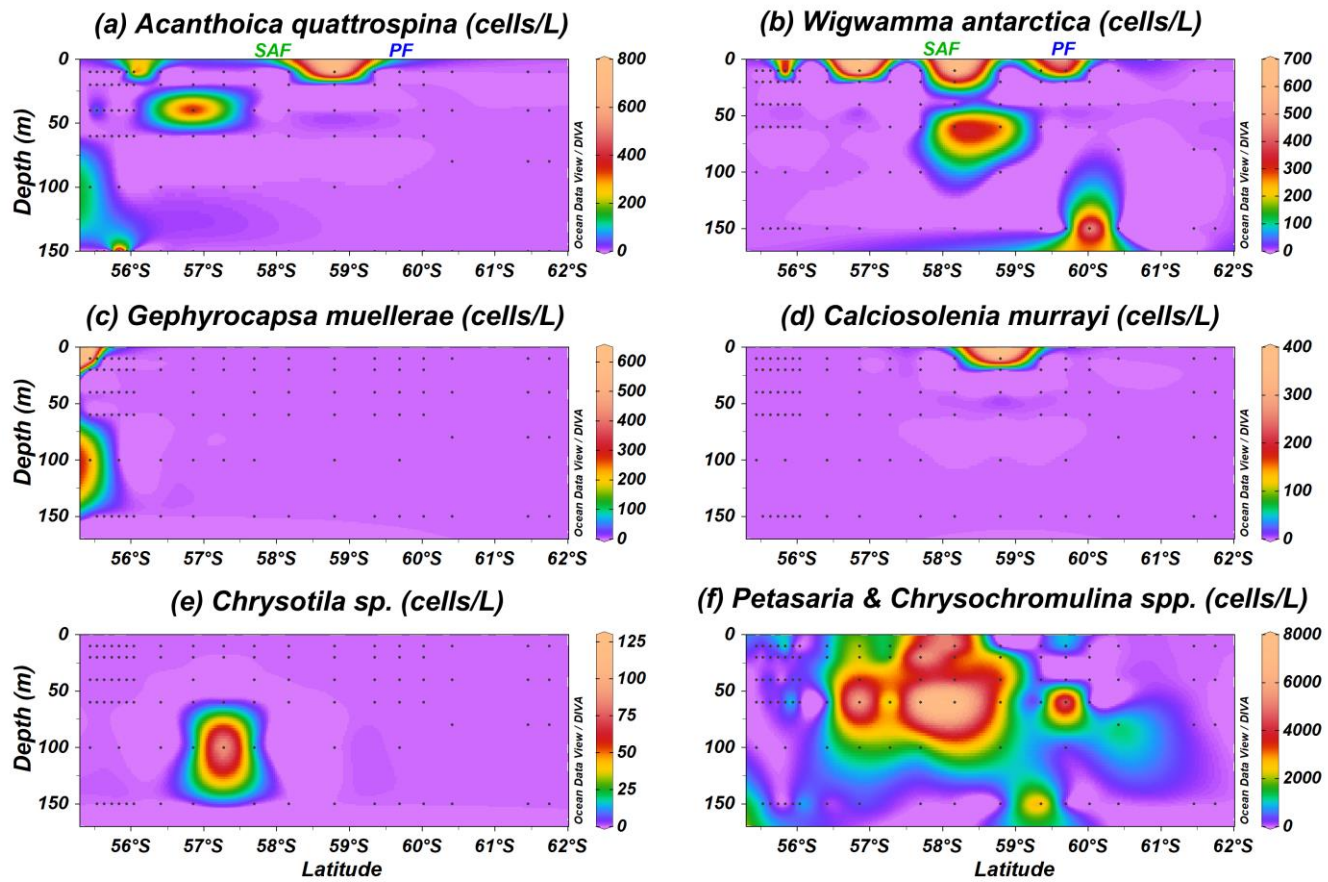
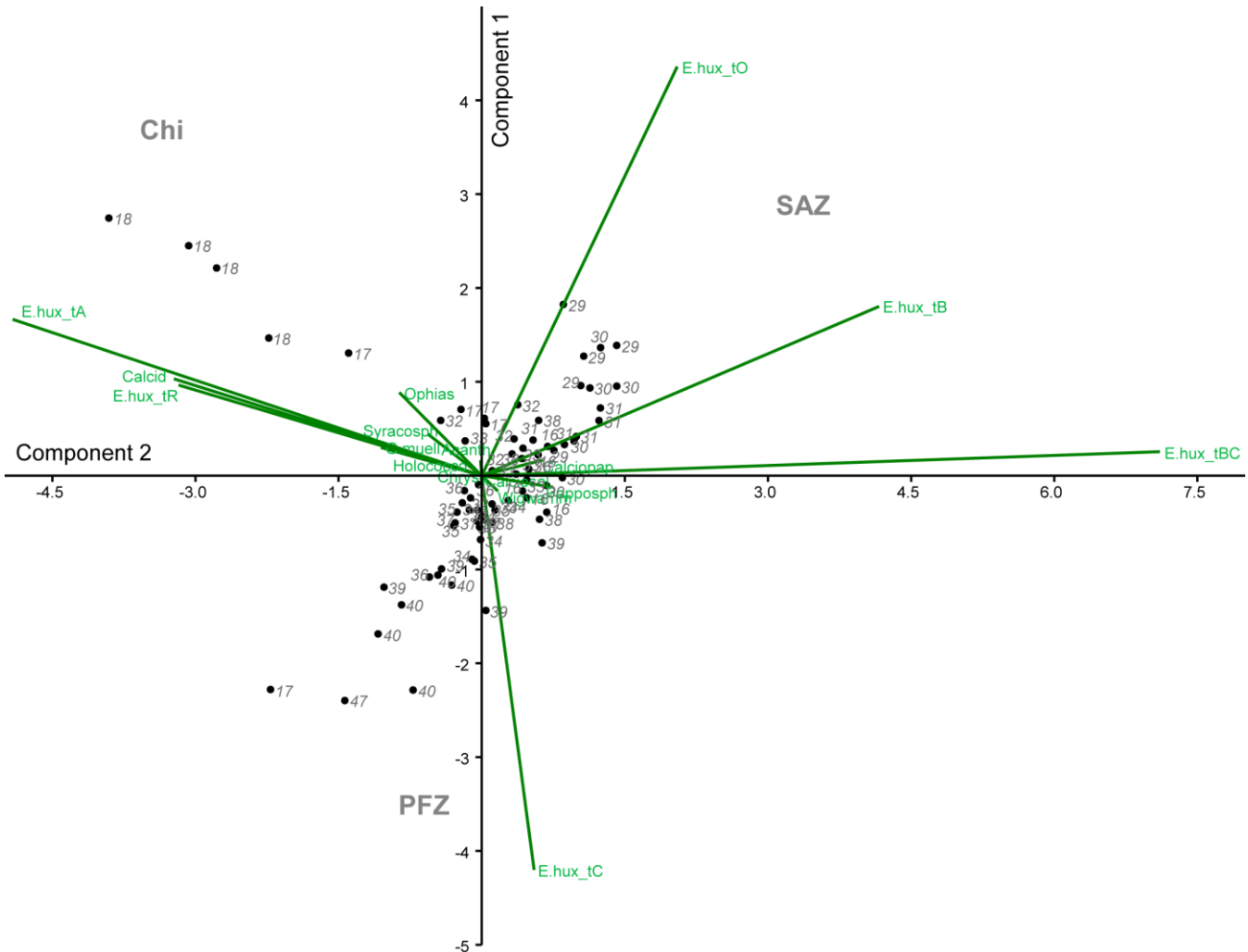


Fig. 7. Location of the PS97 CTD stations studied showing the number of coccospores/L of (a) *Acanthoica quattrospina*, (b) *Wigwamma antarctica*, (c) *Gephyrocapsa muellerae*, (d) *Calciosolenia murrayi*, (e) *Chrysotila* sp., (d) *Petasaria* and *Chrysochromulina* spp. The Subantarctic Front (SAF) and the Polar Front (PF) according to Orsi et al. (1995) are indicated.



**Fig. 8. Principal Component Analysis (PCA) biplot performed on the cocolithophore dataset. The two main components, PC1 (y axis) and PC2 (x axis), cocolithophore taxa, station numbers and the different clusters are indicated. The following abbreviations are used in the figure: E.hux\_tA (E. huxleyi type A), E.hux\_tB (E. huxleyi type B), E.hux\_tBC (E. huxleyi type BC), E.hux\_tC (E. huxleyi type C), E.hux\_tO (E. huxleyi type O), E.hux\_tR (E. huxleyi type R), Calcid (Calcidiscus s.l.), Acanth (Acanthoica quattrospina), Calciopap (Calciopapus caudatus), Calciosol (Calciosolenia murrayi), Chryso (Chrysotila sp.), G.mueller (G. muellerae), Holococco (Holococcolithophores), Ophias (Ophiaster spp.), Pappospha (Papposphaera sp and Pappomonas spp.), Syracosphaera (Syracosphaera spp.), Wigwamm (Wigwamma antarctica), SAZ (subantarctic zone), PFZ (polar front zone) and Chi (Chilean coastal zone).**

5

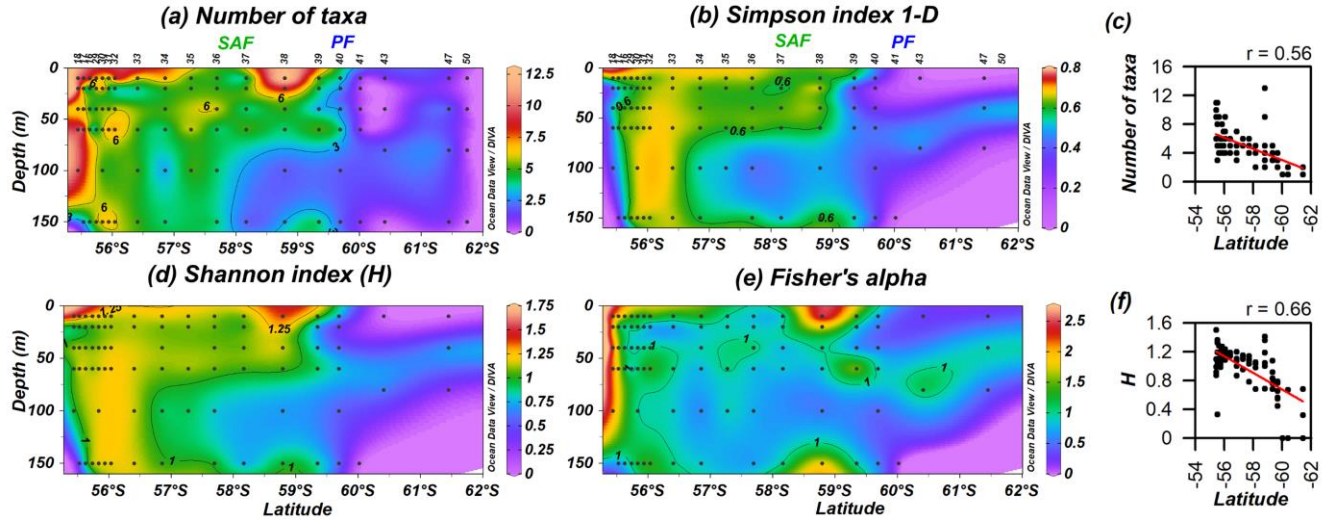
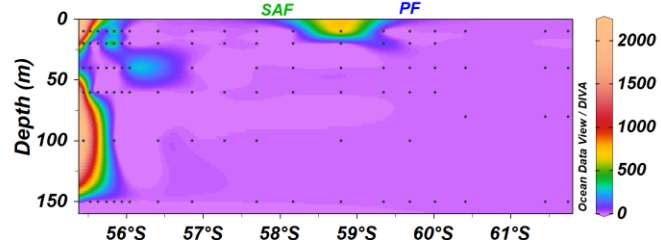
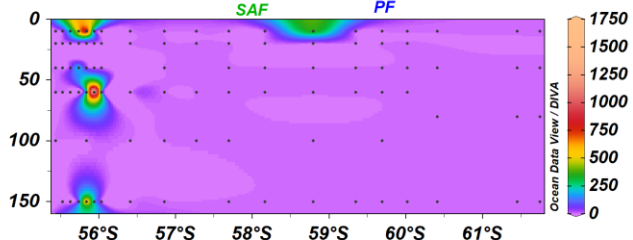


Fig. 9. PS97 latitudinal transects showing coccolithophore diversity: (a) number of taxa, (b) Simpson index 1-D, (c) number of taxa vs latitude, (d) Shannon index (H), (e) Fisher's alpha and (f) H vs latitude. The Subantarctic Front (SAF) and the Polar Front (PF) according to Orsi et al. (1995) are indicated.

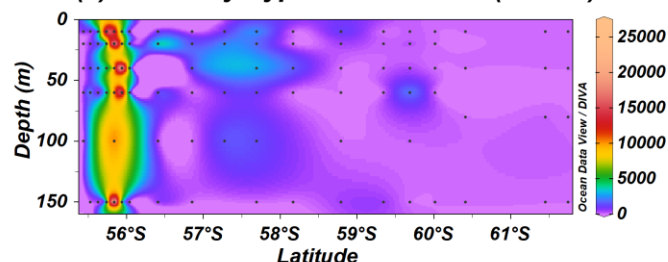
(a) *Emiliania huxleyi* type A calcified -all- (cells/L)



(b) *E. huxleyi* type B calcified (cells/L)



(c) *E. huxleyi* type B/C calcified (cells/L)



(d) *E. huxleyi* type C calcified (cells/L)

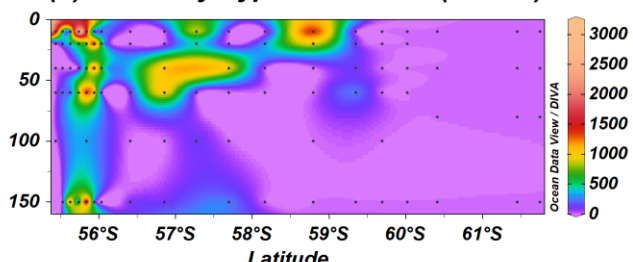


Fig. 10. Location of the PS97 CTD stations studied showing the number of coccospores/L of *Emiliania huxleyi* calcified and overcalcified (a) type A group, (b) type B, (c) type B/C and (d) type C. The Subantarctic Front (SAF) and the Polar Front (PF) according to Orsi et al. (1995) are indicated.

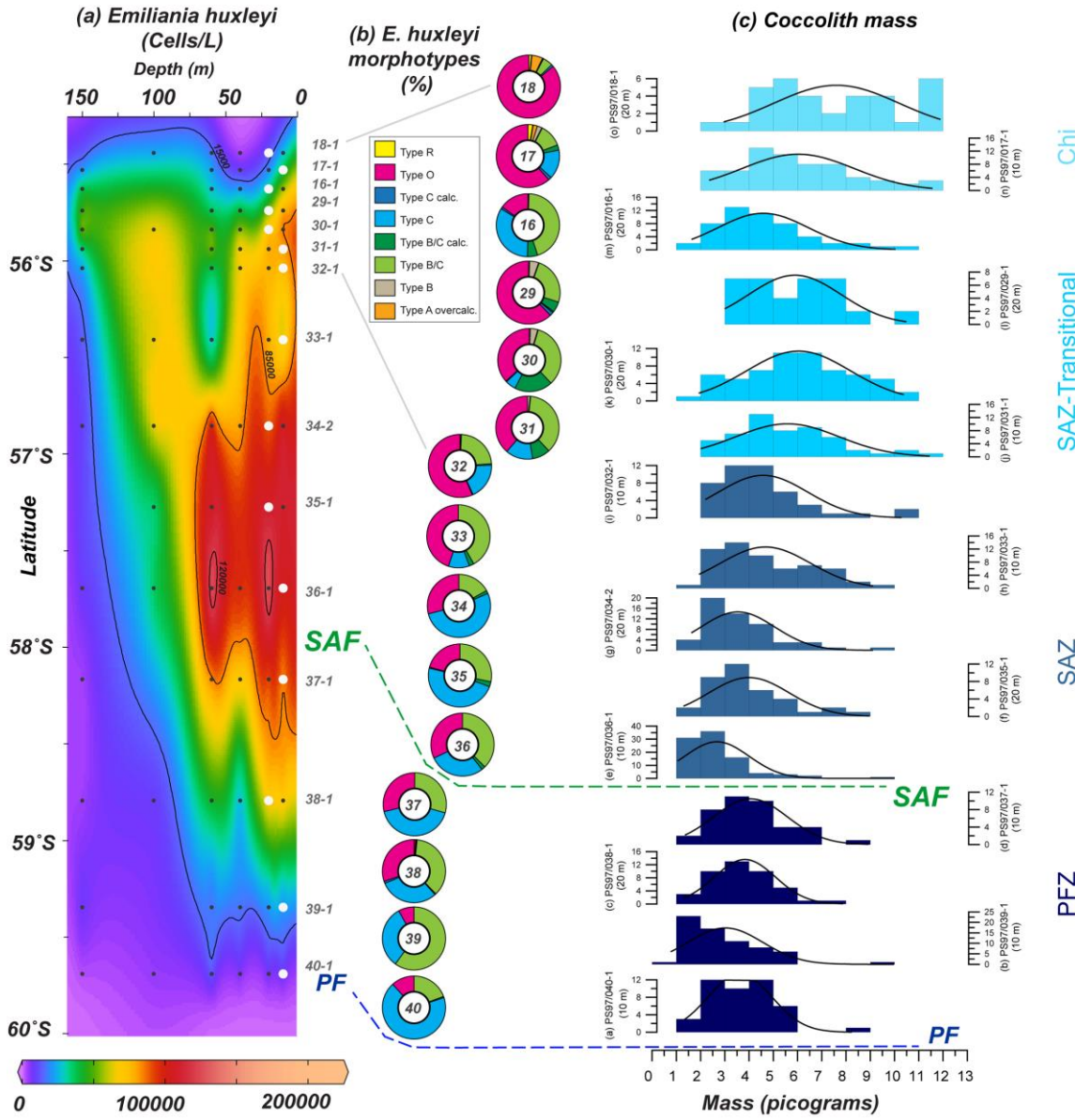
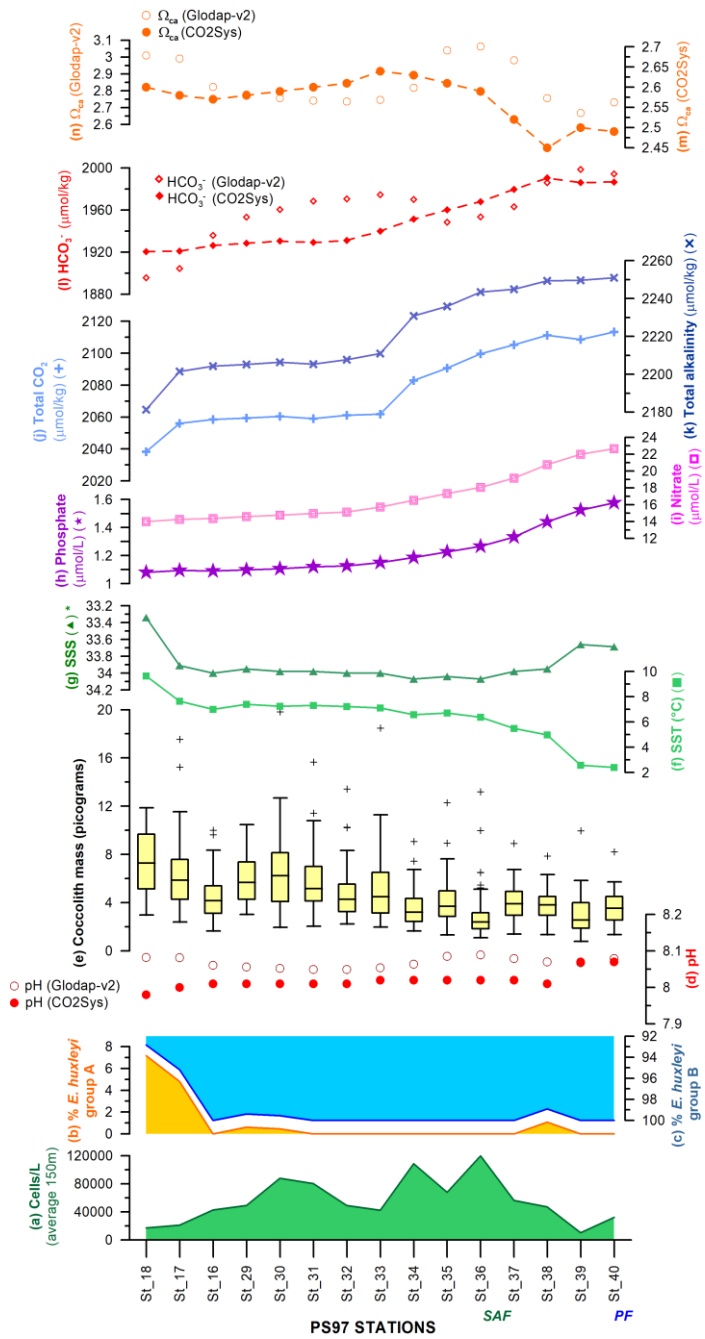
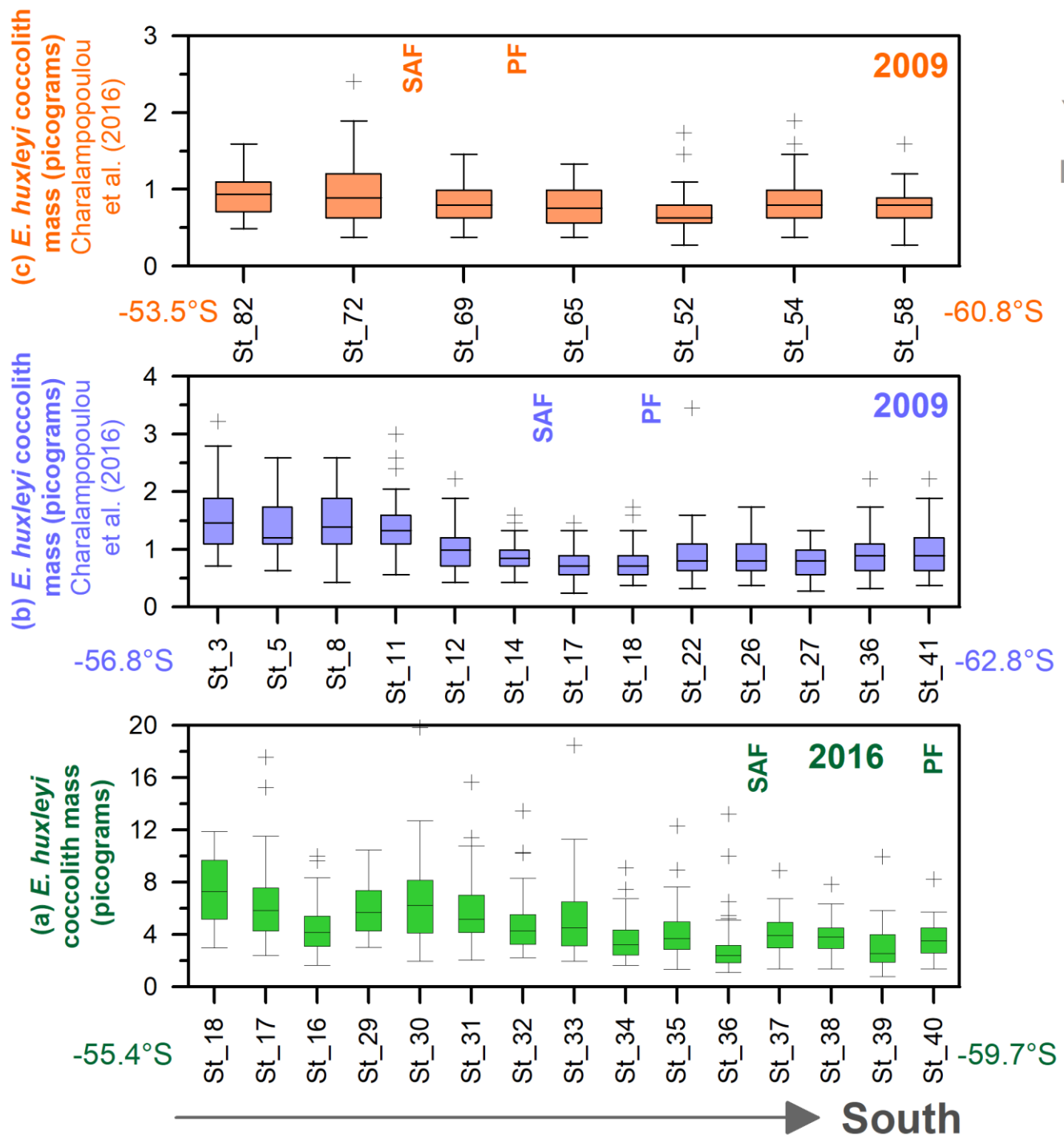


Fig. 11. (a) Location of the PS97 CTD stations between 55.4 and 60°S showing the number of cells/L of *Emiliania huxleyi* from 0 to 150 m. (b) Relative abundance of *E. huxleyi* morphotypes (including the different degree of calcification observed in SEM) in a latitudinal transect (10-20 m, indicated with white dots in (a)), and (c) coccolith mass histograms at those specific locations. Bin size in (c) is 1 picogram and normal distribution fitting line is shown. Station's number, different zones: Chi (Chilean coastal zone), SAZ-transitional (from Chi to open ocean), SAZ (subantarctic zone), PFZ (polar front zone), and the main oceanographic fronts: Subantarctic (SAF) and Polar Fronts (PF) according to Orsi et al. (1995) are indicated.



**Fig. 12.** Latitudinal transect showing on the left hand side: (a) the uppermost 150 m average of cells/L, relative abundance of *E. huxleyi* morphotypes belonging to (b) group A and (c) to group B, (d) pH calculated with different approaches (Pierrot et al., 2006; Key et al., 2015), (e) coccolith mass boxplot (outliers have been indicated with "+"), (f) sea surface temperature (SST, °C) and (g) salinity (\* note the inverted scale) measured in situ (Lamy, 2016). Interpolated (h) phosphate (µmol/L) and (i) nitrate contents (µmol/kg) (Garcia et al., 2014), (j) total alkalinity (µmol/kg) and (k) total CO<sub>2</sub> (µmol/kg) (Goyet et al., 2000), (l) bicarbonate ion (HCO<sub>3</sub><sup>-</sup>, µmol/kg) and (m) calcite saturation state (Ω<sub>Ca</sub>) calculated with different approaches (Pierrot et al., 2006; Key et al., 2015). The subantarctic (SAF) and Polar Fronts (PF) according to Orsi et al. (1995) are indicated.



5 Fig. 13. Drake Passage latitudinal transects from East to West showing boxplot coccolith mass estimates (in picograms): (a) this study, (b) transect at around 68°W Charalampopoulou et al. (2016), (c) transect at around 55-58°W Charalampopoulou et al. (2016). Note that (b, c) have been calculated from Charalampopoulou et al. (2016). Outliers have been indicated with "+" and numbers in the x axes refer to the original station numbers. The approximate location of the Subantarctic (SAF) and Polar Fronts (PF) are shown as well as the year of the sampling.

**Table 1. Classification scheme of *Emiliania huxleyi* morphotypes observed in the present study (modified from Hagino et al. (2011) regarding Young and Westbroek (1991), Cook et al. (2011) and Young et al. (2019)).**

	<i>E. huxleyi</i> morphotype	Morphology of the distal shield	Morphology of the central area	Distal shield length	Comparable morphotypes in the literature
A group	Type A	Moderate-heavily calcified elements	Grill	<4 $\mu$ m	Warm type (McIntyre and Bé, 1967), var. <i>huxleyi</i> (Medlin et al., 1996)
	Type A overcalcified	Moderate-heavily calcified elements	closed or nearly closed	<4 $\mu$ m	Type A overcalcified (Young et al., 2003)
	Type R	<i>Reticulofenestra</i> -like heavily calcified distal shield elements	Covered or nearly covered	<4 $\mu$ m	Type R (Young et al., 2003), (von Dassow et al. 2018)
B group	Type B	Lightly calcified elements	solid plate	$\geq 4$ $\mu$ m	Type B (Young et al., 2003), var. <i>pujosae</i> (Verbeek, 1990) Medlin & Green in Medlin et al. (1996)
	Type B/C	Lightly calcified elements	solid plate	<4 $\mu$ m	Type B/C (Young et al., 2003), var. <i>aurorae</i> (Cook, 2011)
	Type C	Lightly calcified elements	solid plate	<3.5 $\mu$ m	Cold type (McIntyre and Bé, 1967), Type C (Young et al., 2003), var. <i>kleijniae</i> (Medlin et al., 1996)
	Type O	Lightly calcified elements	opened or lamella	variable in size	Subarctic type (Okada and Honjo, 1973), Type B (Hagino et al., 2005)

**Table 2. Summary of the coccolithophore taxa/groups in the studied plankton samples. The presence of each species in the Subantarctic Zone (SAZ), in the Polar Front Zone (PFZ) or in the Antarctic Zone (AZ) is indicated with “+” and with “-” if it is occasional. The station and water depth where the maximum number of cells/L is recorded has been also indicated.**

Coccolithophore taxa / groups	SAZ	PFZ	AZ	Max. (cells/L)	Station	Depth (m)
<i>Acanthoica quattrospina</i>	+	-		0.7*10 <sup>3</sup>	PS97/038-1	10
<i>Calcidiscus</i> s.l.	+	-		1.4*10 <sup>3</sup>	PS97/038-1	10
<i>Chrysotila</i> sp.	-			0.1*10 <sup>3</sup>	PS97/035-1	100
<i>Calciosolenia murrayi</i>	+	-		0.3*10 <sup>3</sup>	PS97/038-1	10
<i>Calcioppapus caudatus</i>	+	-		5.3*10 <sup>3</sup>	PS97/038-1	10
<i>Emiliania huxleyi</i> type A (incl. overcalcified)	+	-		2.1*10 <sup>3</sup>	PS97/018-1	100
<i>Emiliania huxleyi</i> type R	+	-		0.9*10 <sup>3</sup>	PS97/029-1	20
<i>Emiliania huxleyi</i> type B	+	-		7.4*10 <sup>3</sup>	PS97/030-1	10
<i>Emiliania huxleyi</i> type B/C	+	+	-	74.0*10 <sup>3</sup>	PS97/034-1	150
<i>Emiliania huxleyi</i> type C	+	+	-	103.2*10 <sup>3</sup>	PS97/036-2	60
<i>Emiliania huxleyi</i> Type O (incl. lamella)	+	+	-	76.2*10 <sup>3</sup>	PS97/018-1	60
<i>Gephyrocapsa muellerae</i>	+			0.6*10 <sup>3</sup>	PS97/036-1	10
Holococcolithophores	+			1.0*10 <sup>3</sup>	PS97/038-1	60
<i>Ophiaster</i> spp. (incl. <i>hydroideus</i> & <i>reductus</i> )	+	-		10.2*10 <sup>3</sup>	PS97/035-1	10
<i>Papposphaera</i> sp.	-			0.2*10 <sup>3</sup>	PS97/038-1	60
<i>Pappomonas</i> spp. (incl. sp. 1 & 5)	+	+		1.4*10 <sup>3</sup>	PS97/038-1	20
<i>Syracosphaera</i> spp. (incl. <i>dilatata</i> , <i>corolla</i> , <i>marginaporata</i> , <i>pulchra</i> )	+	-		2.8*10 <sup>3</sup>	PS97/034-2	10
<i>Wigwamma antarctica</i>	-	+	-	0.7*10 <sup>3</sup>	PS97/034-2	10

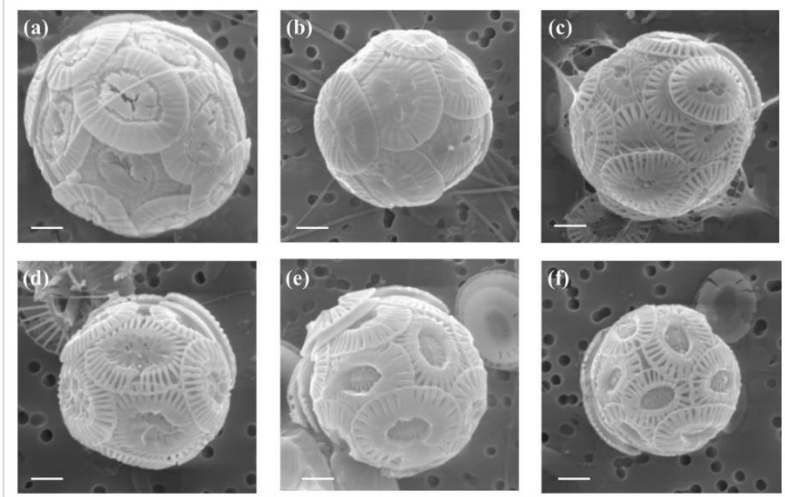
**Table 3. Correlation matrix between Principal component (PC) scores and the environmental variables. Significant Pearson correlation coefficients are indicated in bold (p<0.05)**

Variables	PC 1	PC 2
SST	<b>0.77</b>	-0.01
SSS	<b>-0.23</b>	<b>0.66</b>
Density	<b>-0.77</b>	<b>0.41</b>
Oxygen	<b>-0.70</b>	-0.02
Fluorometer	-0.13	-0.13
Phosphate	<b>-0.70</b>	-0.21
Nitrate	<b>-0.70</b>	-0.20
Silicate	<b>-0.61</b>	-0.22

**Table 4. Correlation matrix between mean / median coccolith values and the environmental variables. Significant Pearson correlation coefficients are indicated in bold ( $p<0.05$ ). Measurements in situ and calculated values are indicated.**

Environmental variables		Mean coccolith mass (pg)	Median coccolith mass (pg)
In situ	Temperature	<b>0.75</b>	<b>0.71</b>
	Salinity	-0.35	-0.37
	Fluorescence	0.10	0.13
Calculated	Phosphate	<b>-0.71</b>	<b>-0.66</b>
	Nitrate	<b>-0.75</b>	<b>-0.70</b>
	Silicate	-0.35	-0.31
	Total CO <sub>2</sub>	<b>-0.82</b>	<b>-0.77</b>
	Total Alkalinity	<b>-0.85</b>	<b>-0.81</b>
	HCO <sub>3</sub> <sup>-</sup> Glodap-v2	<b>-0.68</b>	<b>-0.66</b>
	HCO <sub>3</sub> <sup>-</sup> CO2Sys	<b>-0.81</b>	<b>-0.75</b>
	pH Glodap-v2	-0.25	-0.22
	pH CO2Sys	<b>-0.70</b>	<b>-0.69</b>
	CO <sub>3</sub> <sup>2-</sup> Glodap-v2	0.09	0.08
	CO <sub>3</sub> <sup>2-</sup> CO2Sys	0.40	0.32
	Ω <sub>ca</sub> Glodap-v2	0.10	0.10
	Ω <sub>ca</sub> CO2Sys	0.39	0.31

*Emiliania huxleyi* type A group



*Emiliania huxleyi* type B group

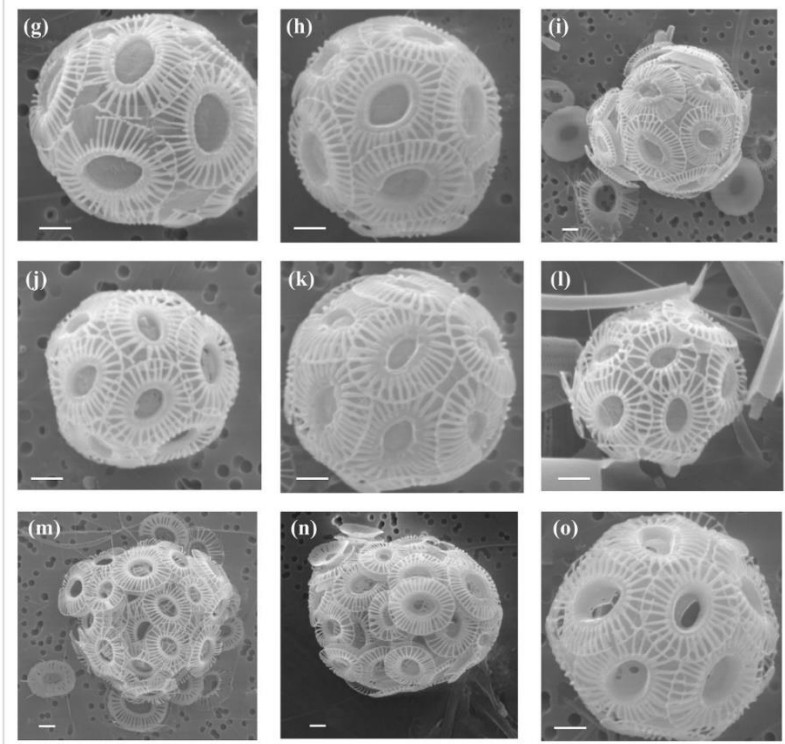
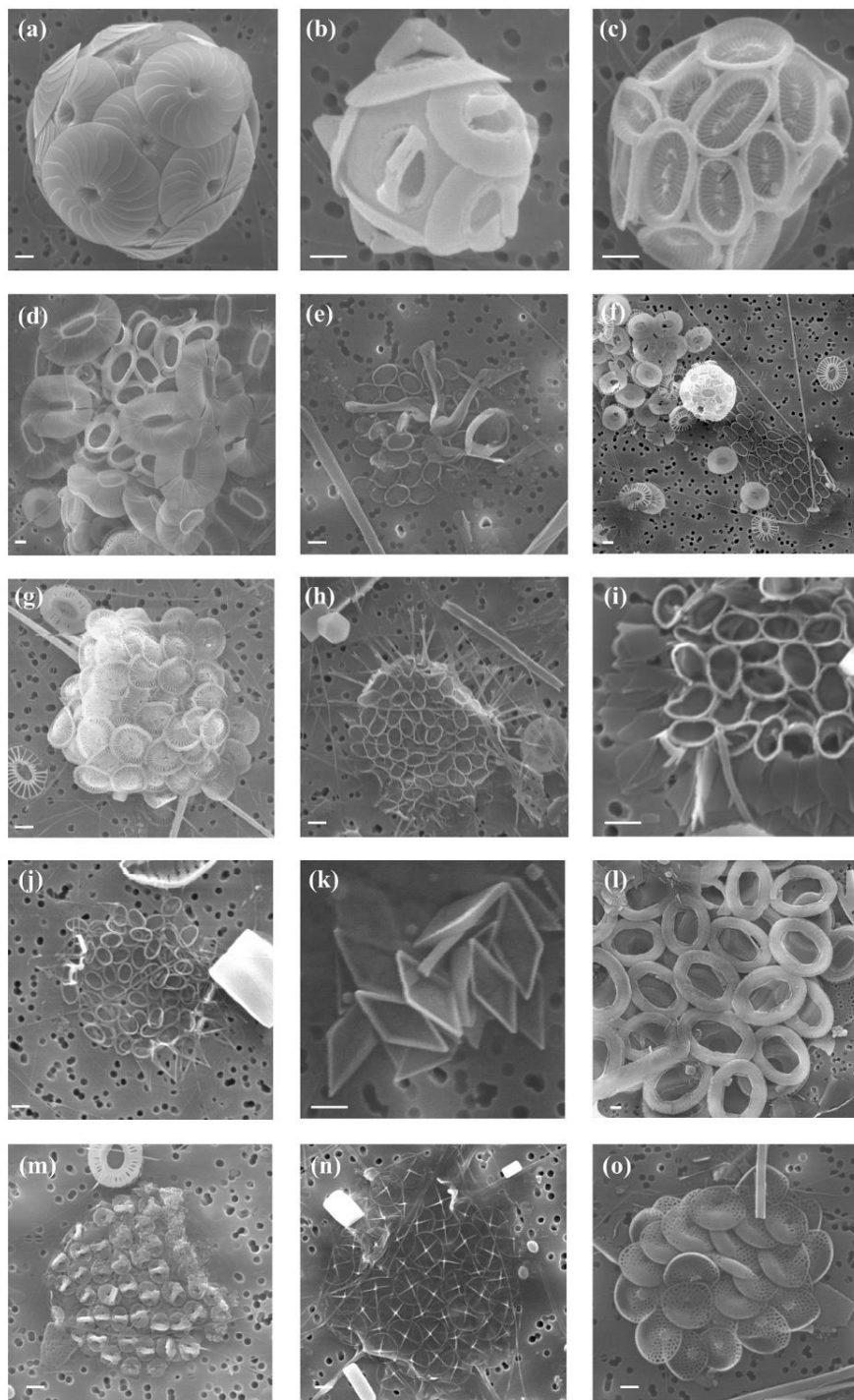


Plate 1. Specimens of *Emiliania huxleyi*. Group A includes (a) type R, sample PS97/018-1 at 10 m water depth; (b) type A overcalcified, PS97/018-1 at 60 m; (c) type A overcalcified, PS97/018-1 at 100 m; (d) type A calcified, PS97/018-1 at 60 m; (e) type A calcified PS97/018-1 at 20 m; (f) type A slightly calcified, PS97/018-1 at 60 m.

5

*Emiliania huxleyi* group B includes: (g) type B PS97/016-1 at 5 m; (h) type B PS97/029-1 at 60 m; (i) type B calcified, PS97/29-1 at 150 m; (j) type B/C PS97/016-1 at 10 m; (k) type B/C slightly calcified PS97/030-1 at 150 m; (l) type C PS97/043-1, at 10 m; (m) type O - opened-, PS97/032-1 at 10 m; (n) type O -lamella-, PS97/038-1 at 10 m; (o) type O -lamella- PS97/017-1 at 60 m. The scale bar indicates 1  $\mu$ m.



5 **Plate 2. Other taxa present in the study area. Specimens of (a) *Calcidiscus leptoporus* s.s., sample PS97/016-1 at 5 m water depth; (b) *Gephyrocapsa muellerae*, PS97/018-1 at 10 m; (c) *Syracosphaera dilatata*, PS97/32-1 at 10 m; (d) *Syracosphaera corolla*, PS97/38-1 at 10 m; (e) *Ophiaster hydroideus*, PS97/38-1 at 10 m; (f) *Calcipappus caudatus* and *Emiliania huxleyi*, PS97/34-2 at 10 m; (g) *Acanthoica quattrospina*, PS97/32-1 at 10 m; (h) *Papposphaera sagittifera* sp., PS97/38-1 at 20 m; (i) *Papposphaera* cf. *heldalii*, PS97/30-1 at 40 m; (j) *Wigwamma antarctica*, PS97/39-1 at 10 m; (k) *Calciosolenia* sp., PS97/38-1 at 10 m; (l) *Chrysotila* sp., PS97/35-1 at 100 m; (m) *Syracosphaera strigilis* HOL, PS97/17-1 at 40 m; (n) *Chrysochromulina* sp.; (o) *Petasaria heterolepis* sp., PS97/38-1 at 40 m. The scale bar indicates 1  $\mu$ m.**